Cortico-cortical long-range connectivity: Anatomical data from mouse and monkey

Almut Schüz

Max Planck Institute for Biological Cybernetics, Tübingen, Germany

Sao Paulo, 26.11.2015

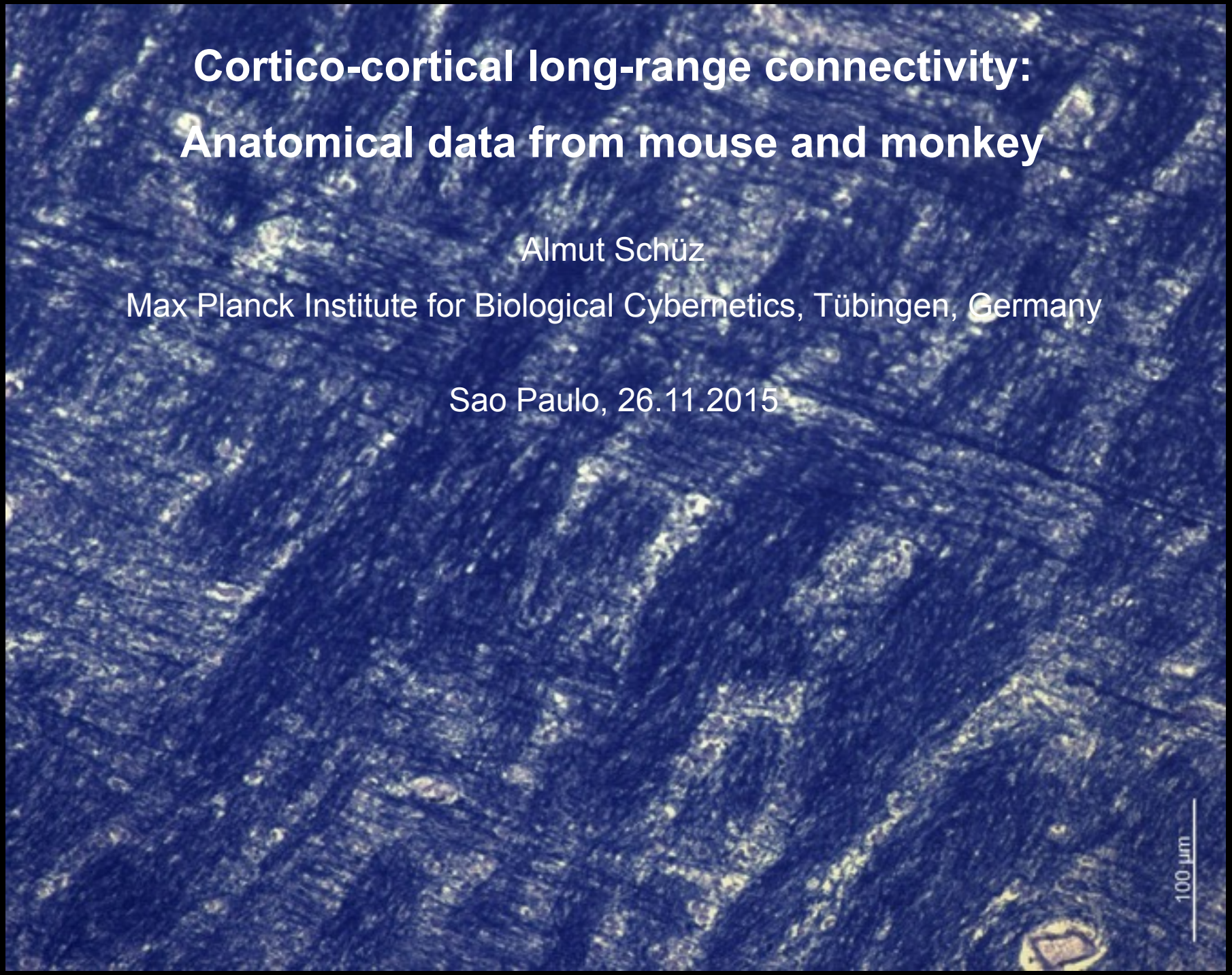

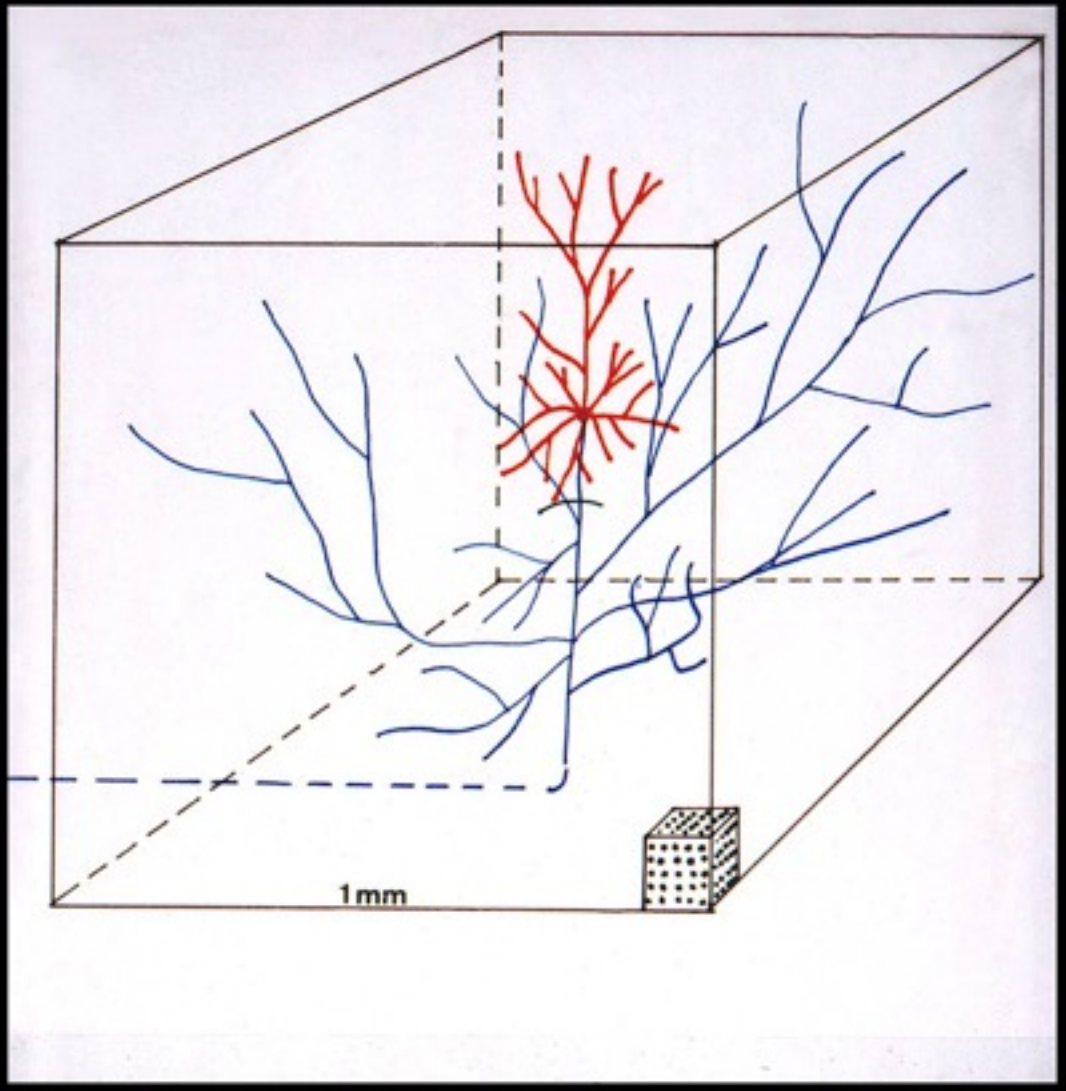
1mm

Cortico-cortial long-range connections

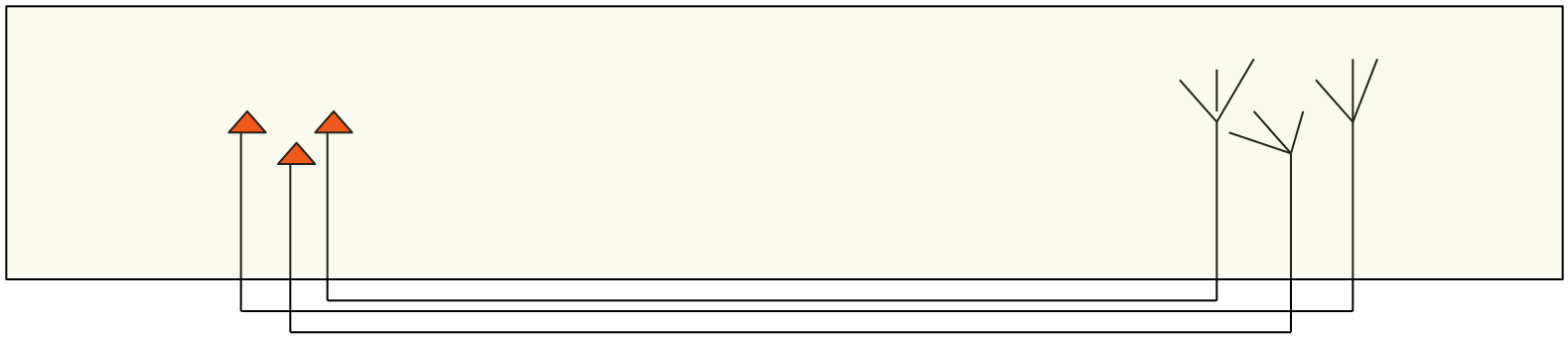

Tracer methods

Square root compartments

Global connectivity in the mouse cortex

Patchy connections in large brains

Human cortical white matter

Tracer methods

Using axonal transport:

Slow transport: up to 30 mm/day
Fast transport: up to 40 cm/day

anterograde tracing

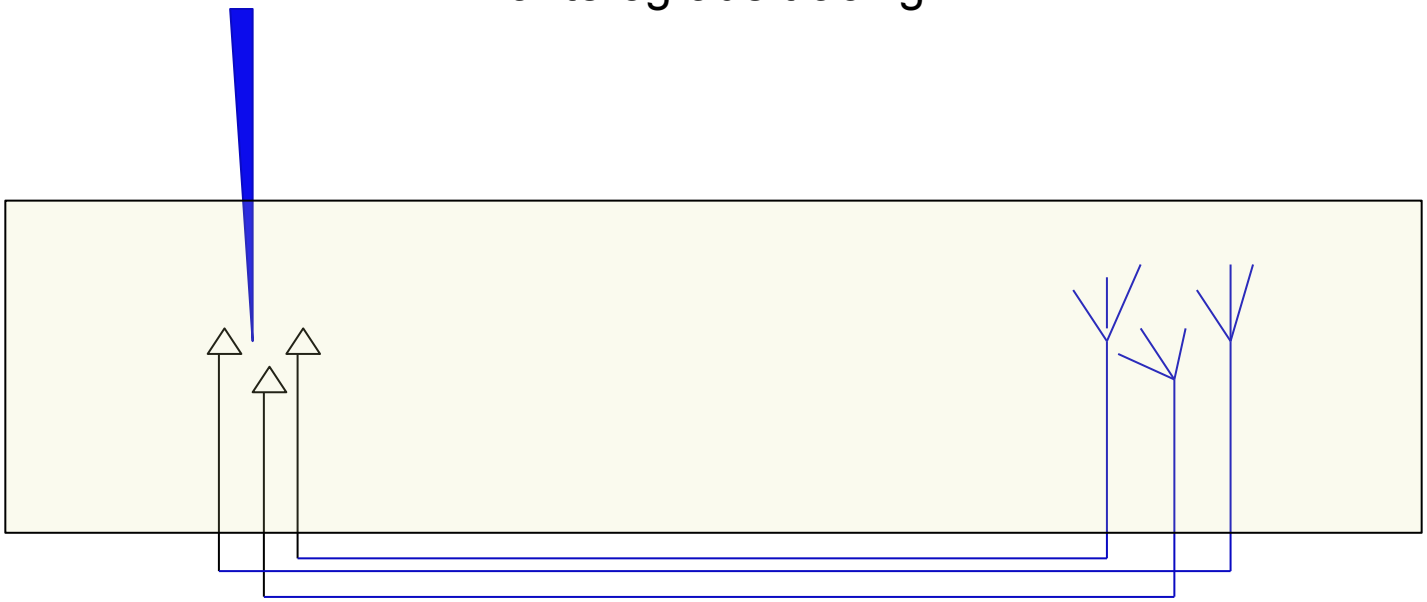

where to?

Anterograde: radioactive amino acids

phaseolus vulgaris (PHA-L)

WGA (wheet germ agglutinine)

biotinylated dextran amine (BDA)

Anterograde staining after Injection of the tracer BDA

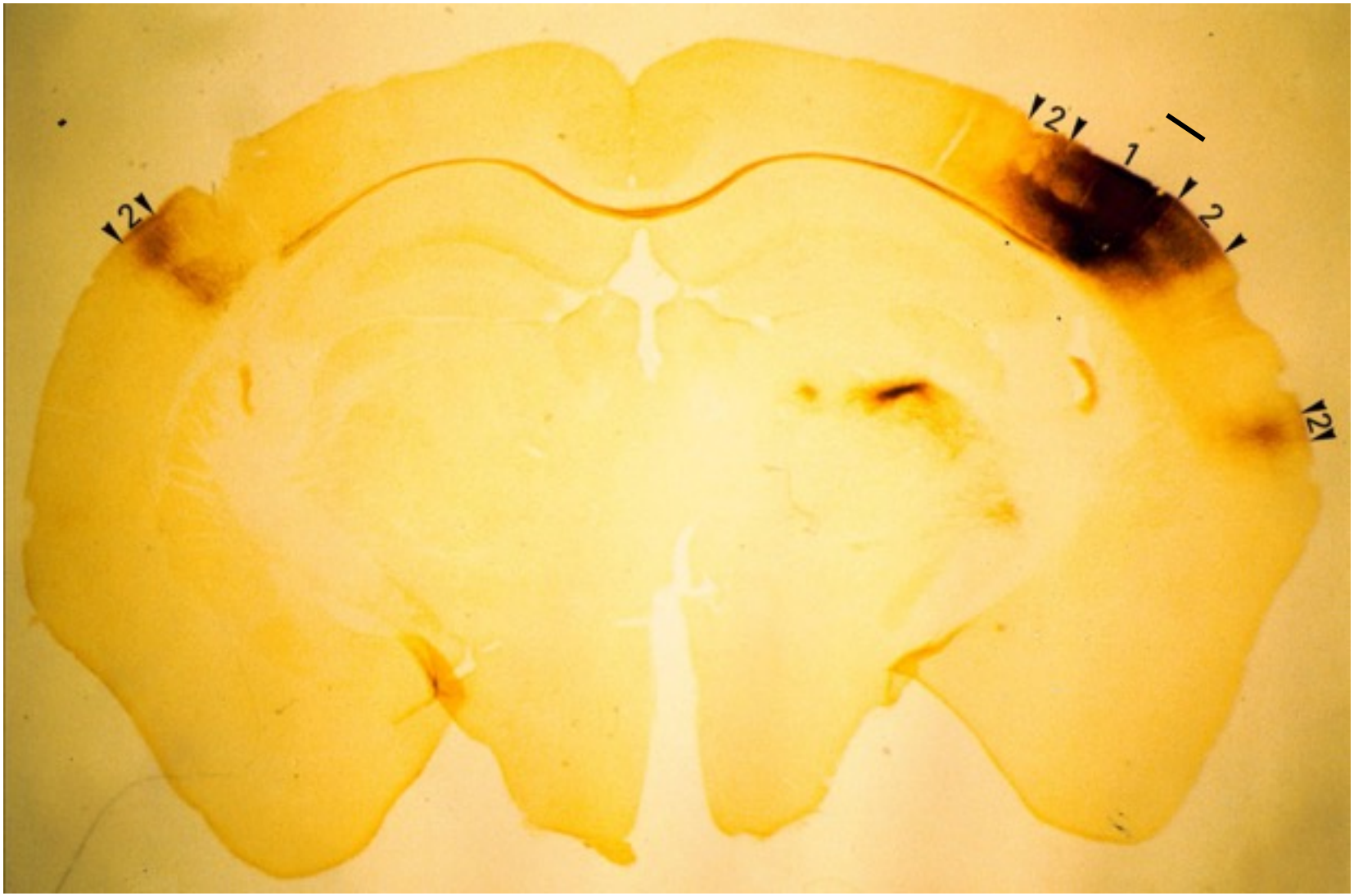

From Schüz et al., 2005

retrograde tracing

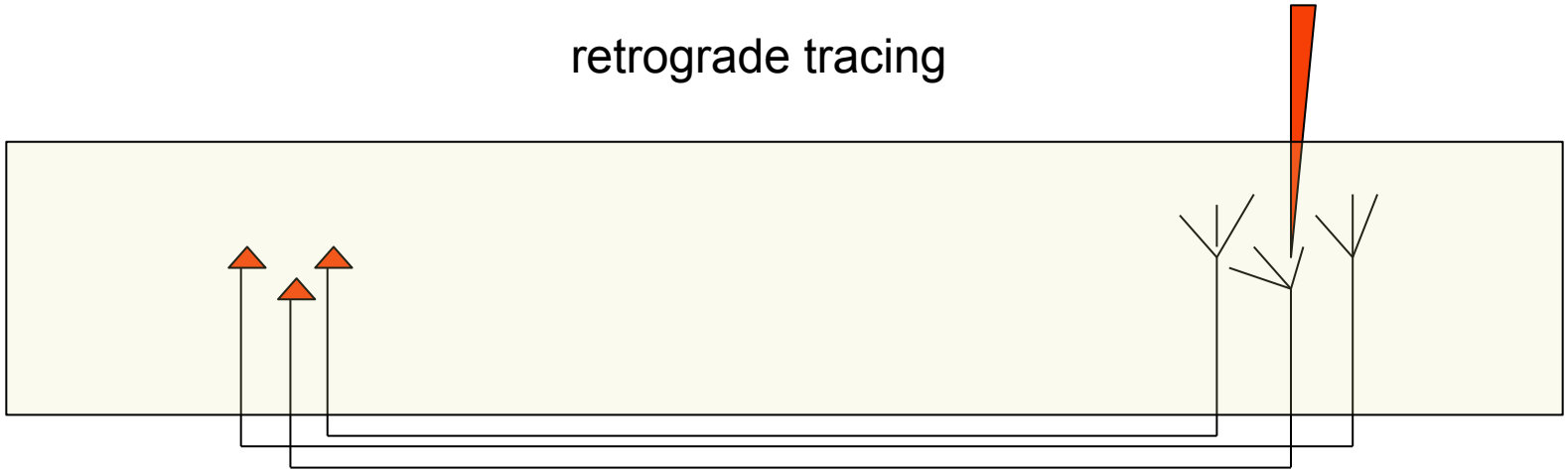

where from?

Retrograde: fluorescent dyes (e.g. Rhodamin, Fast Blue, Fluorogold)

horse-radish peroxidase (HRP) (predominantly retrogr.)

Both directions: biocytin (biotin + Lysin)

neurotrophic viruses (e.g. Herpes simplex or Rabies) – also transsynaptically

Fluorescent dyes, retrograde staining, after injection in Area 17 (light blue) and 41 (greenish blue)

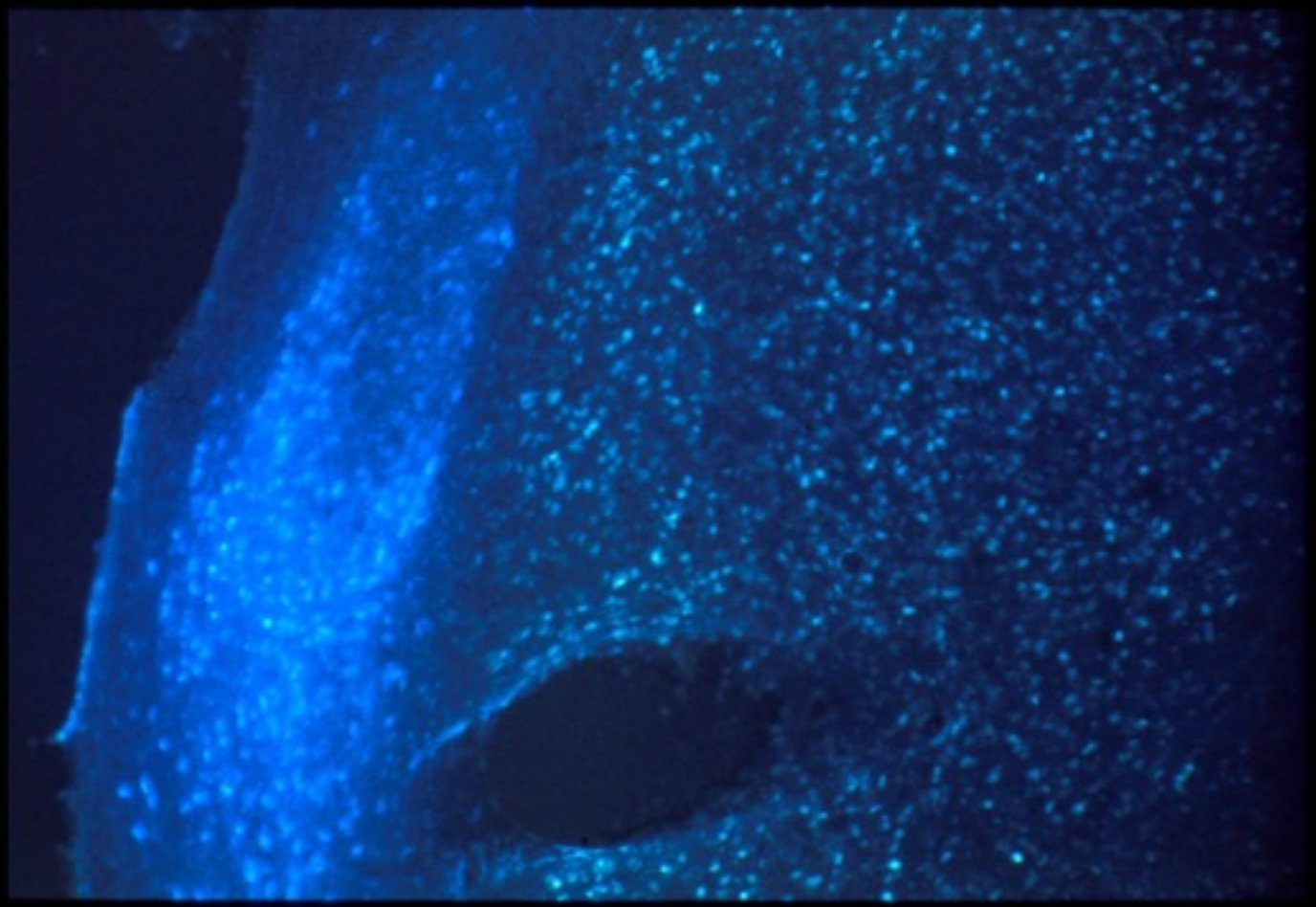

Retrograde Tracer, horseradisch peroxidase

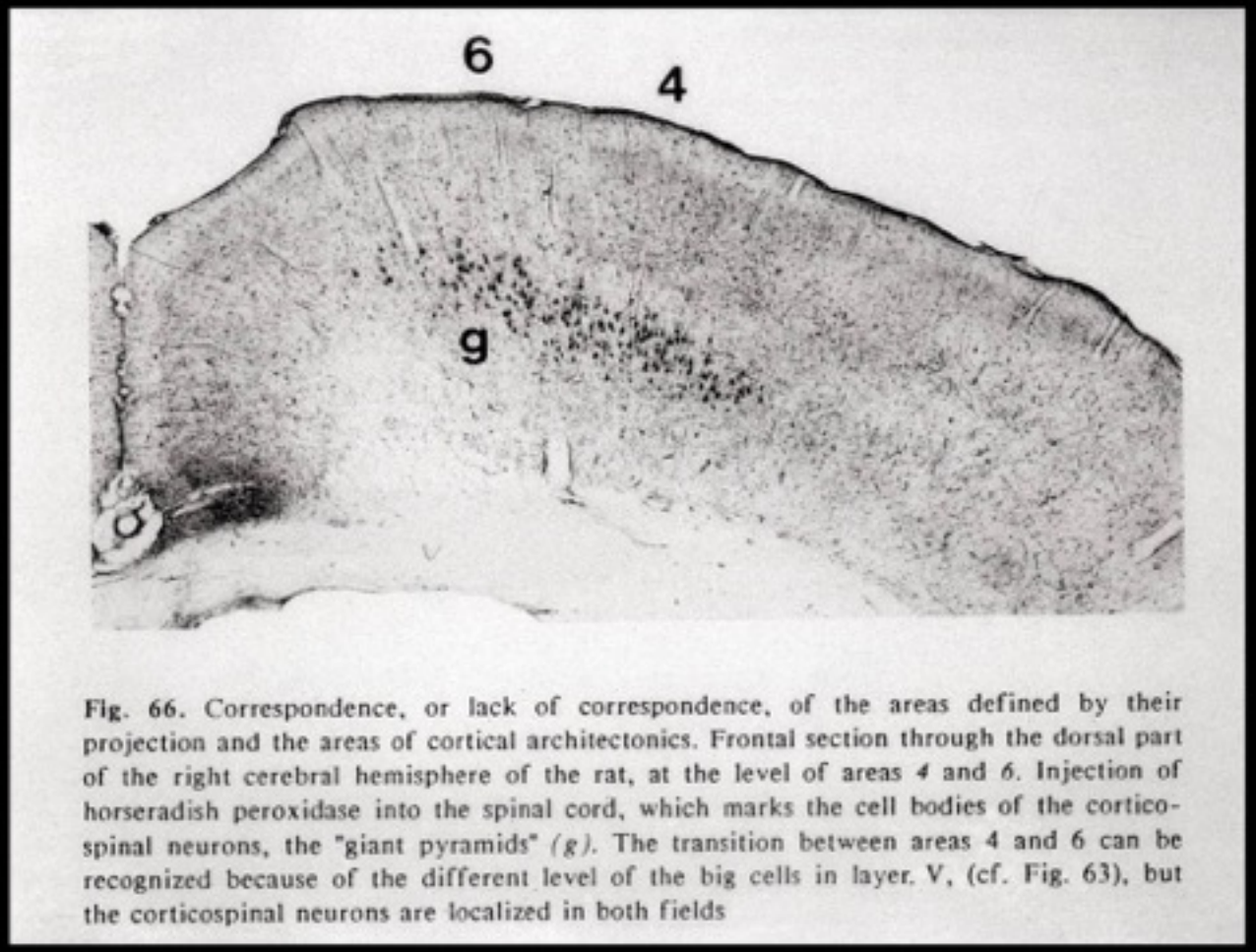

Fig. 66. Correspondence, or lack of correspondence, of the areas defined by their projection and the areas of cortical architectonics. Frontal section through the dorsal part of the right cerebral hemisphere of the rat, at the level of areas *4* and *6*. Injection of horseradish peroxidase into the spinal cord, which marks the cell bodies of the cortico-spinal neurons, the "giant pyramids" *(g)*. The transition between areas 4 and 6 can be recognized because of the different level of the big cells in layer. V, (cf. Fig. 63), but the corticospinal neurons are localized in both fields

From Braitenberg and Schüz, 1998

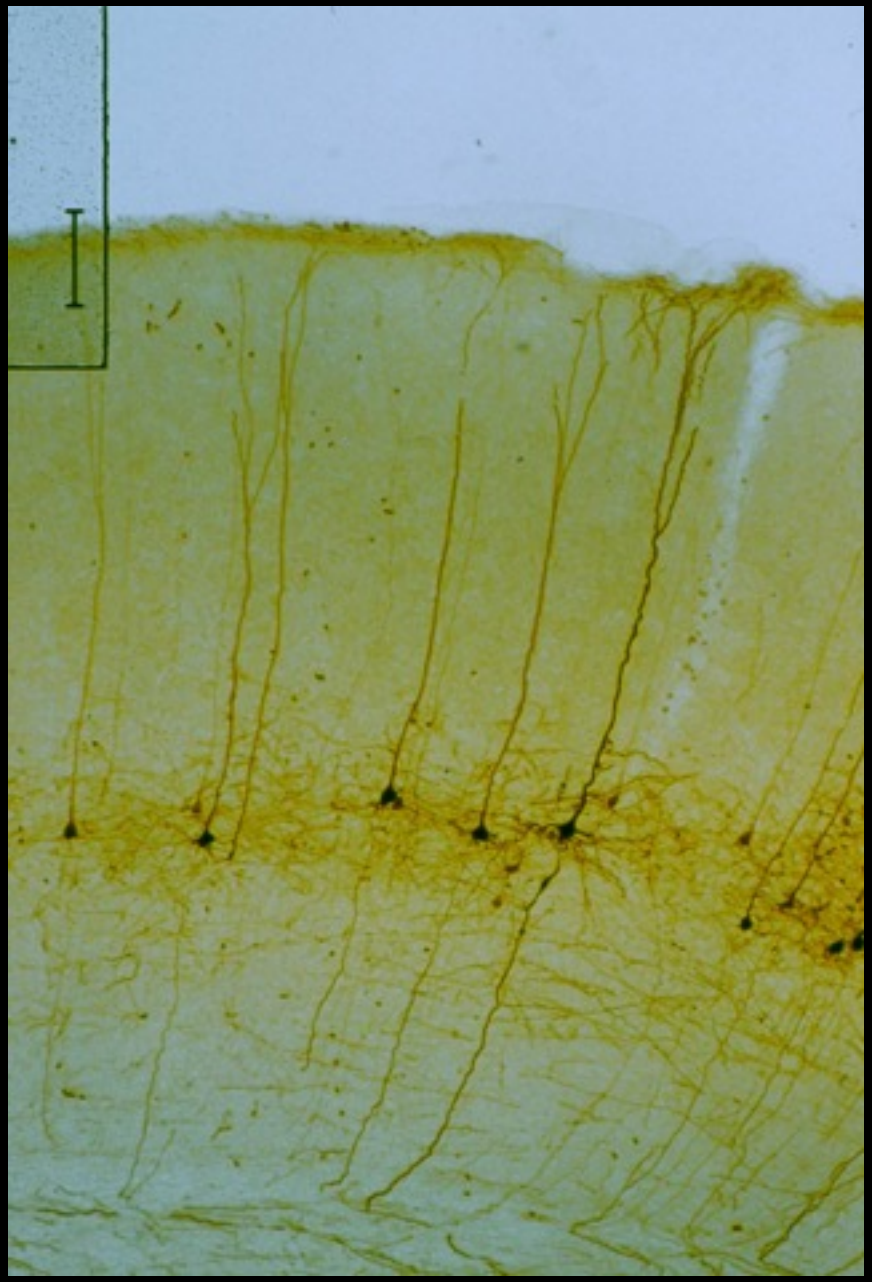

Retrogradely
stained pyramidal cells,
mouse cortex (BDA)

Tracing in the human brain post-mortem

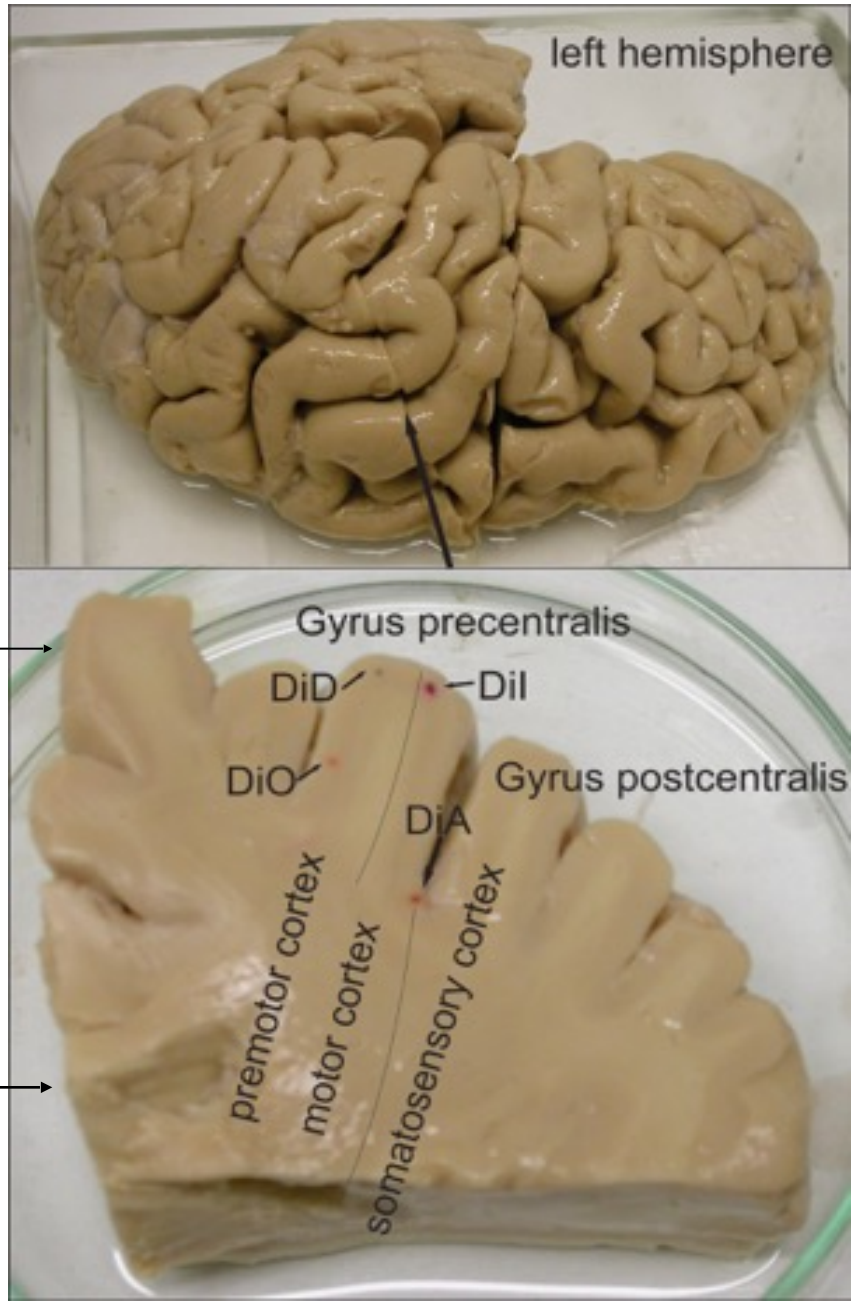

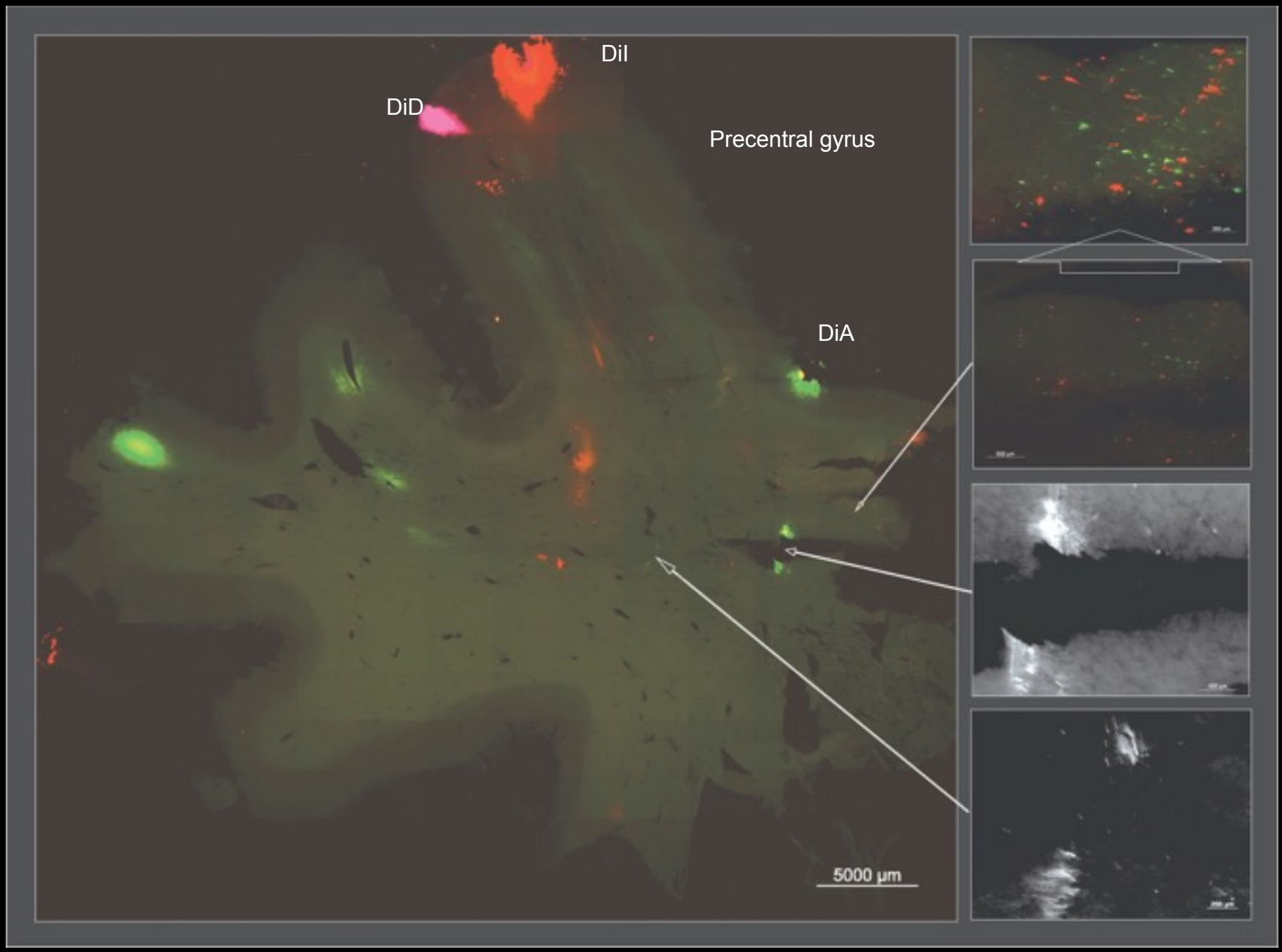
DiI
DiD
Precentral gyrus
DiA
5000 µm

Tracers usable in vivo in magnetic resonance imaging (MRI):

Manganese (activity dependent; transsynaptic)

Biocytin

Magnetic resonance imaging and histology of biocytin (type L3) tracer with Gd

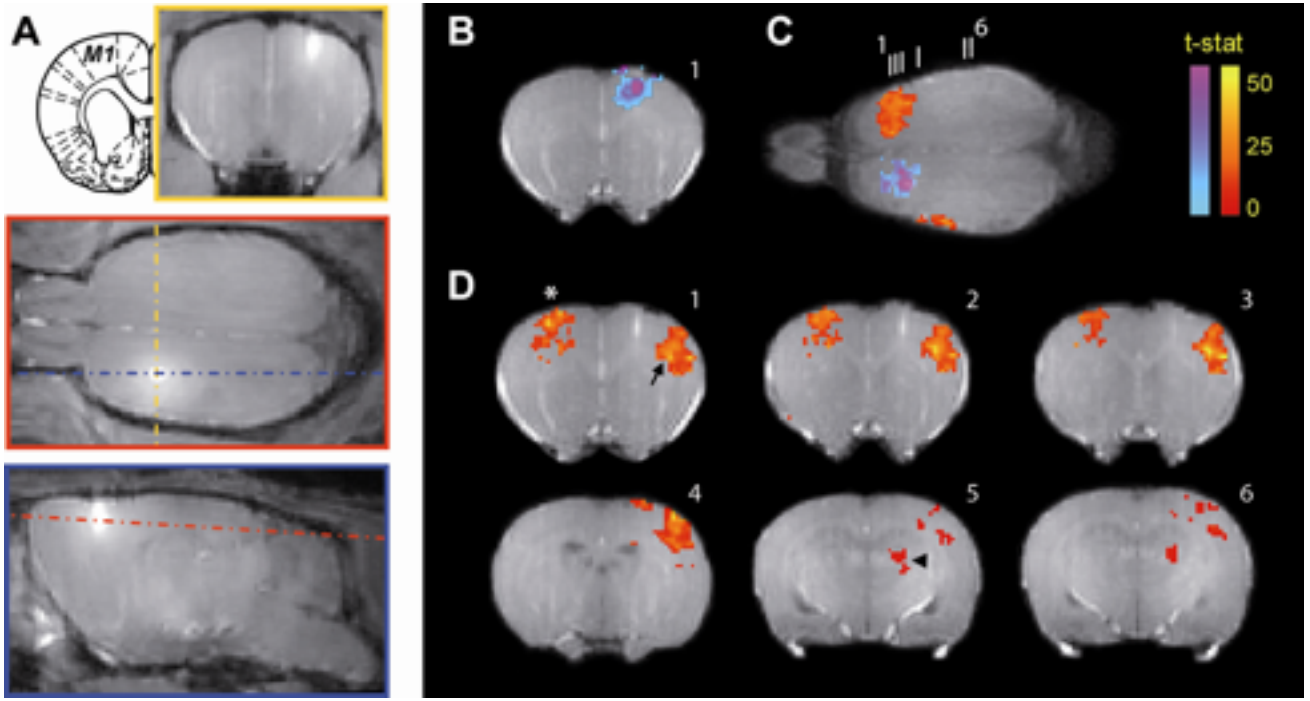

From: Mishra et al. (2011) Biocytin-Derived MRI Contrast Agent for Longitudinal Brain Connectivity Studies

Surface area of the cortex (1 hemisphere)

mouse – monkey – human

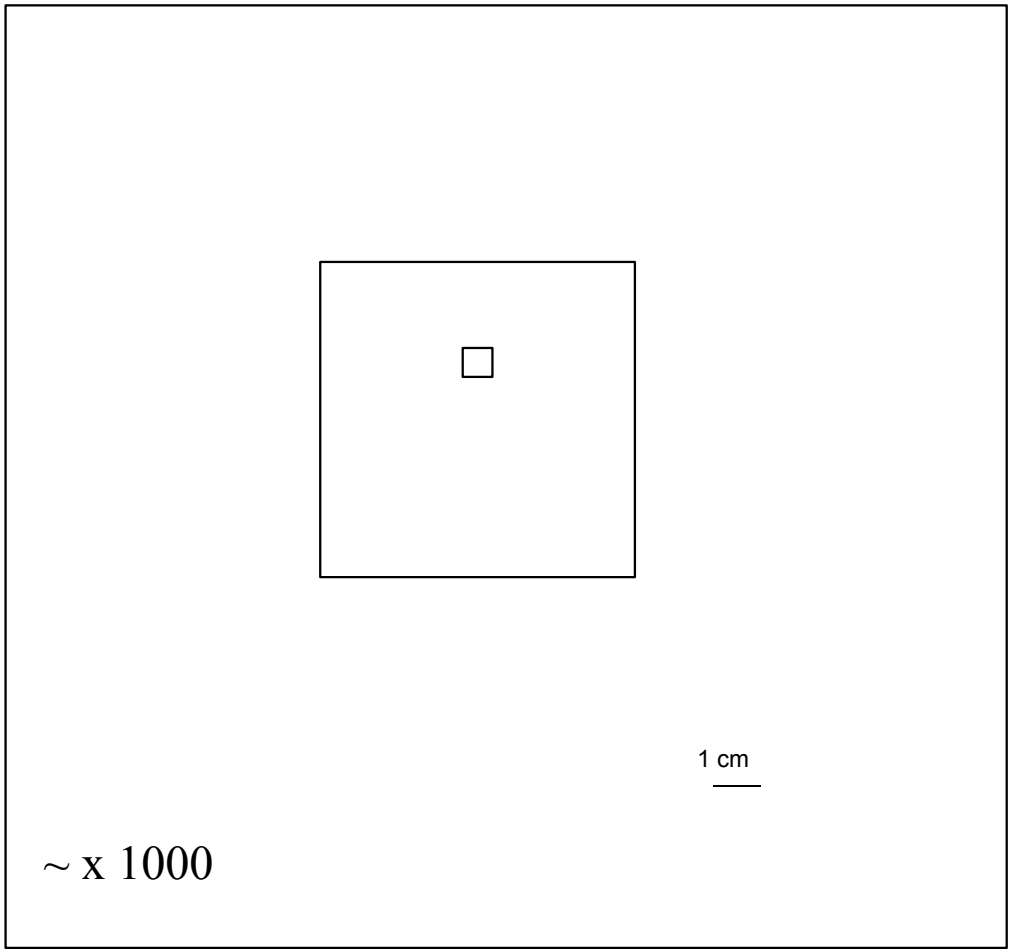

An abstract scheme for a full set of cortico-cortical connections:

Parcellation into „square root compartments“
(Braitenberg, 1978)

An abstract scheme for a full set of cortico-cortical connections:

Parcellation into „square root compartments“
(Braitenberg, 1978)

N total number of neurons

$\sqrt{N}$ compartments

Each containing $\sqrt{N}$ neurons

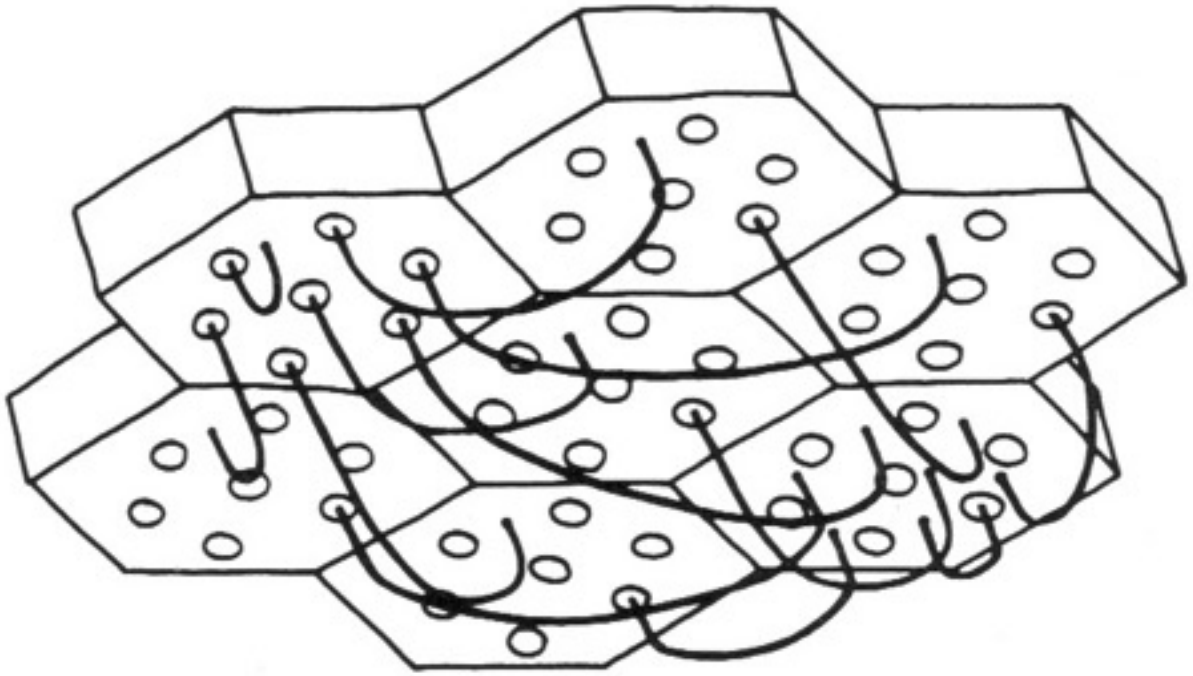

Braitenberg 1978

Mouse cortex:

$N \approx 8\text{-}9 \times 10^6$/hemisphere

$\sqrt{N} \approx 3000$ compartments,
diameter about 0.17 mm

Human cortex:

$N \approx 10^{10}$/hemisphere

$\sqrt{N} \approx 100\,000$ compartments,
diameter ca. 1 mm

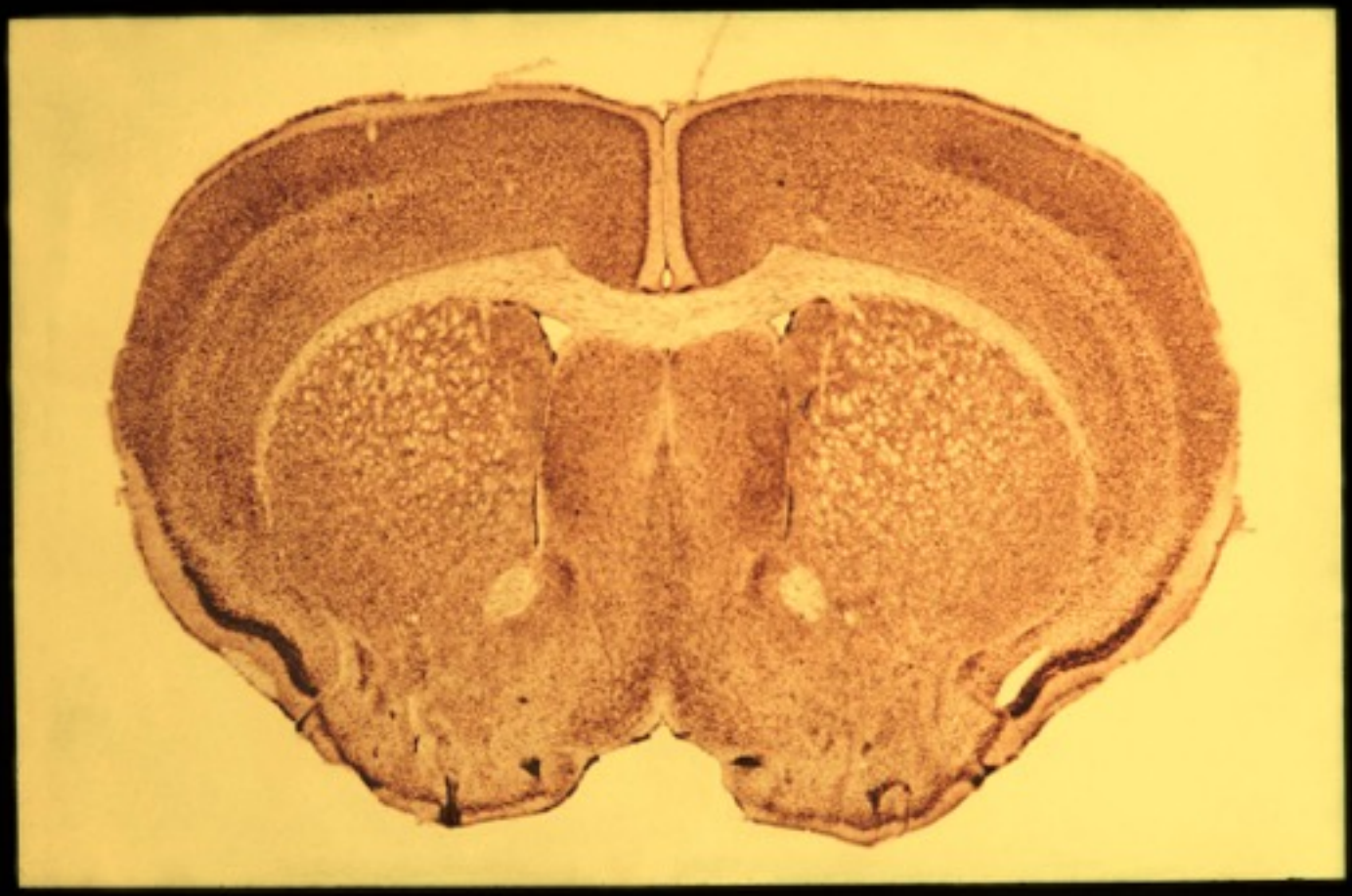

Mouse,
Nissl-stain,
Coronal
section

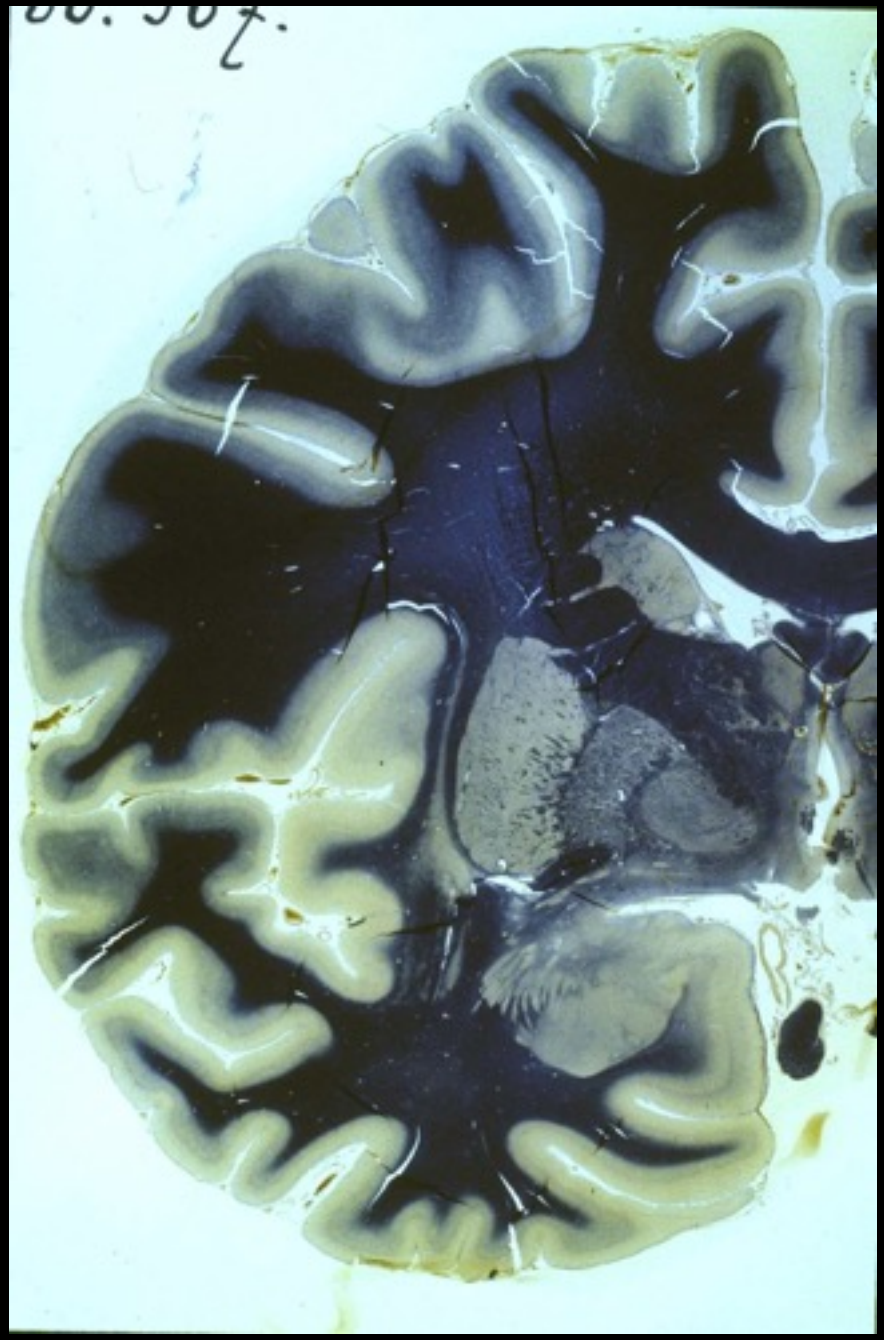

Section: Max Planck Institute for Brain Res. (Frankfurt)

Foto:
Bernhard Hellwig (Tübingen)

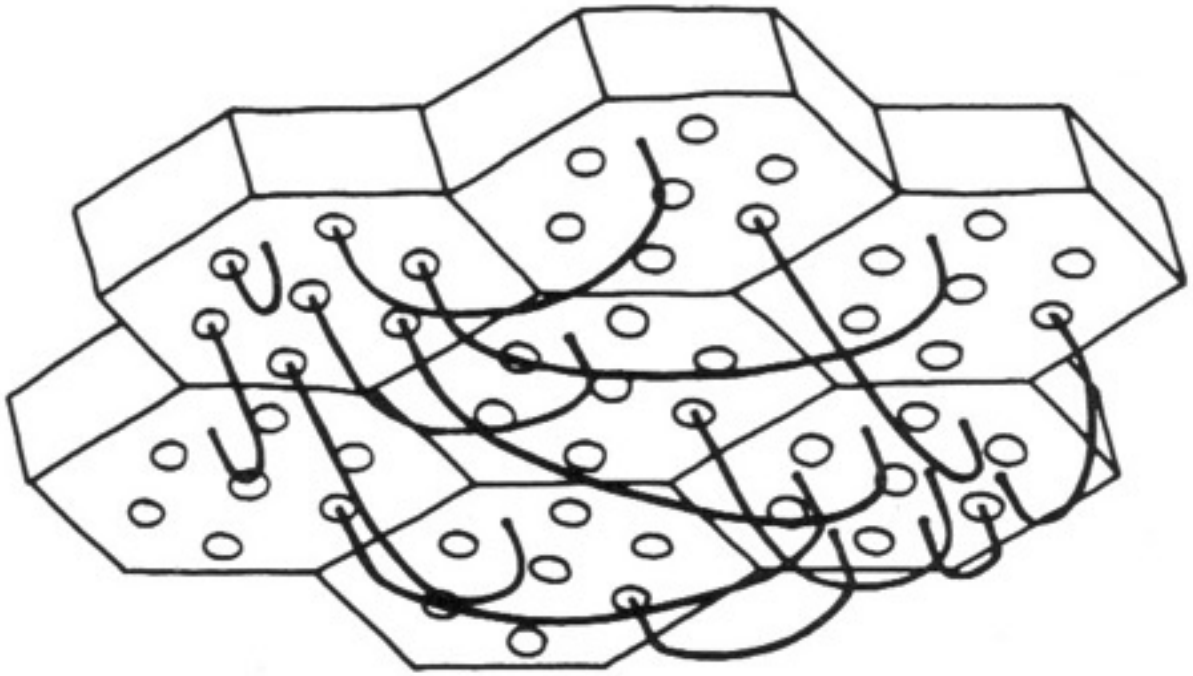

Braitenberg 1978

Global connectivity of the cortex, a tracer study in the mouse

Together with Daniel Liewald, Denis Chaimow and Monika Dortenmann

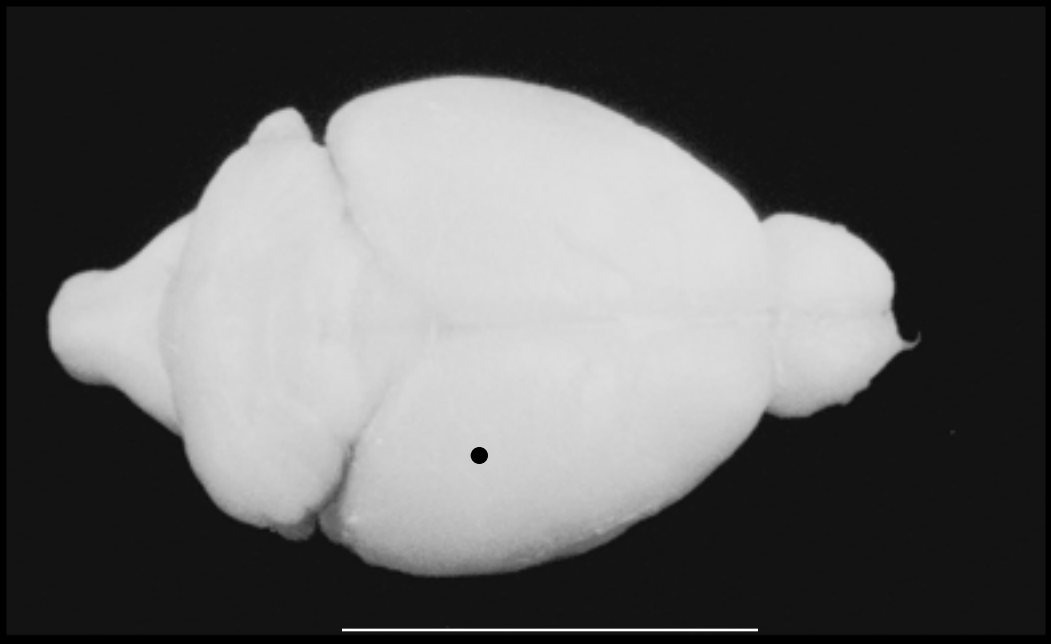

1 cm

Anterograde staining after Injection of the tracer BDA

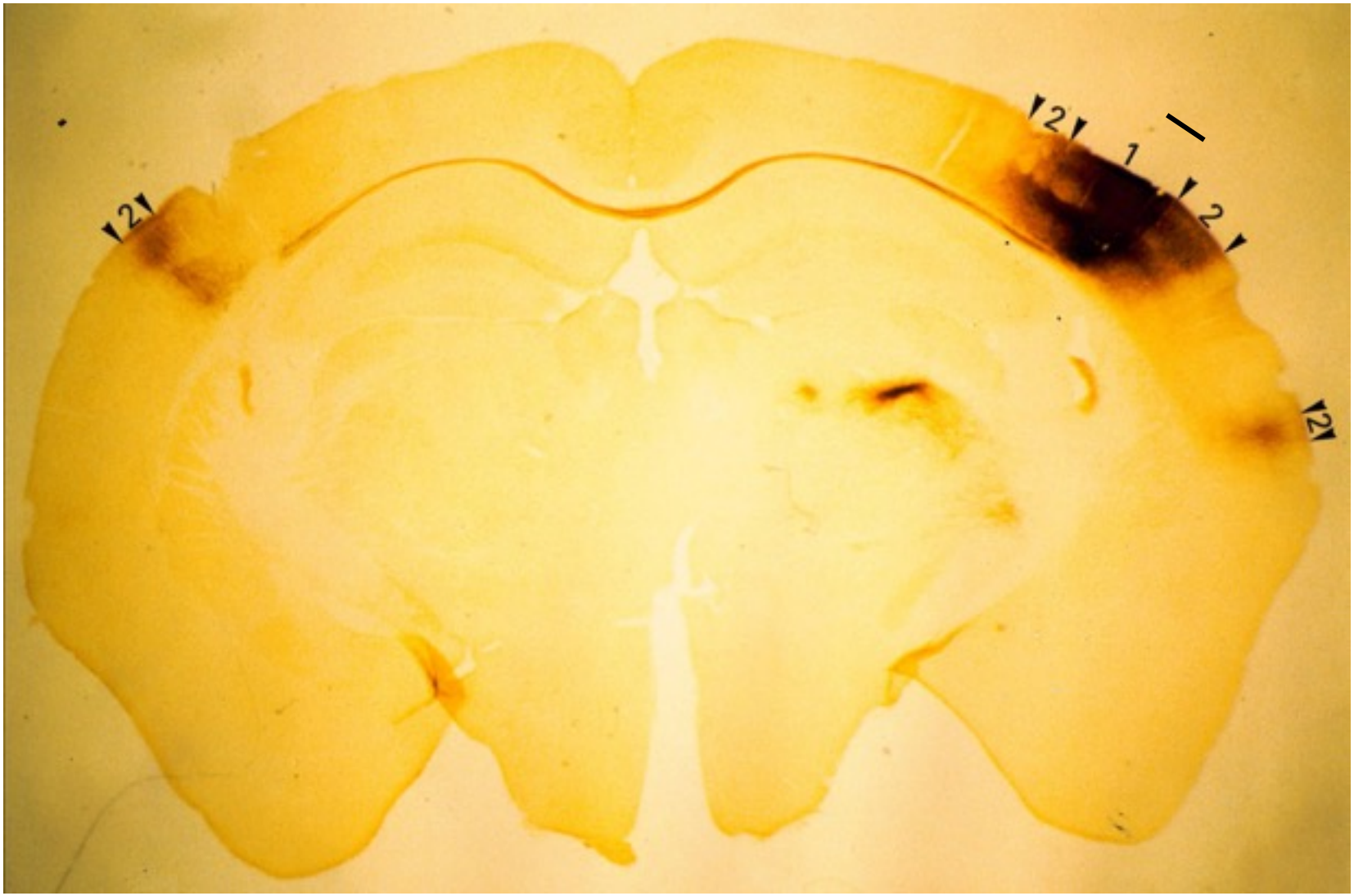

From Schüz et al., 2005

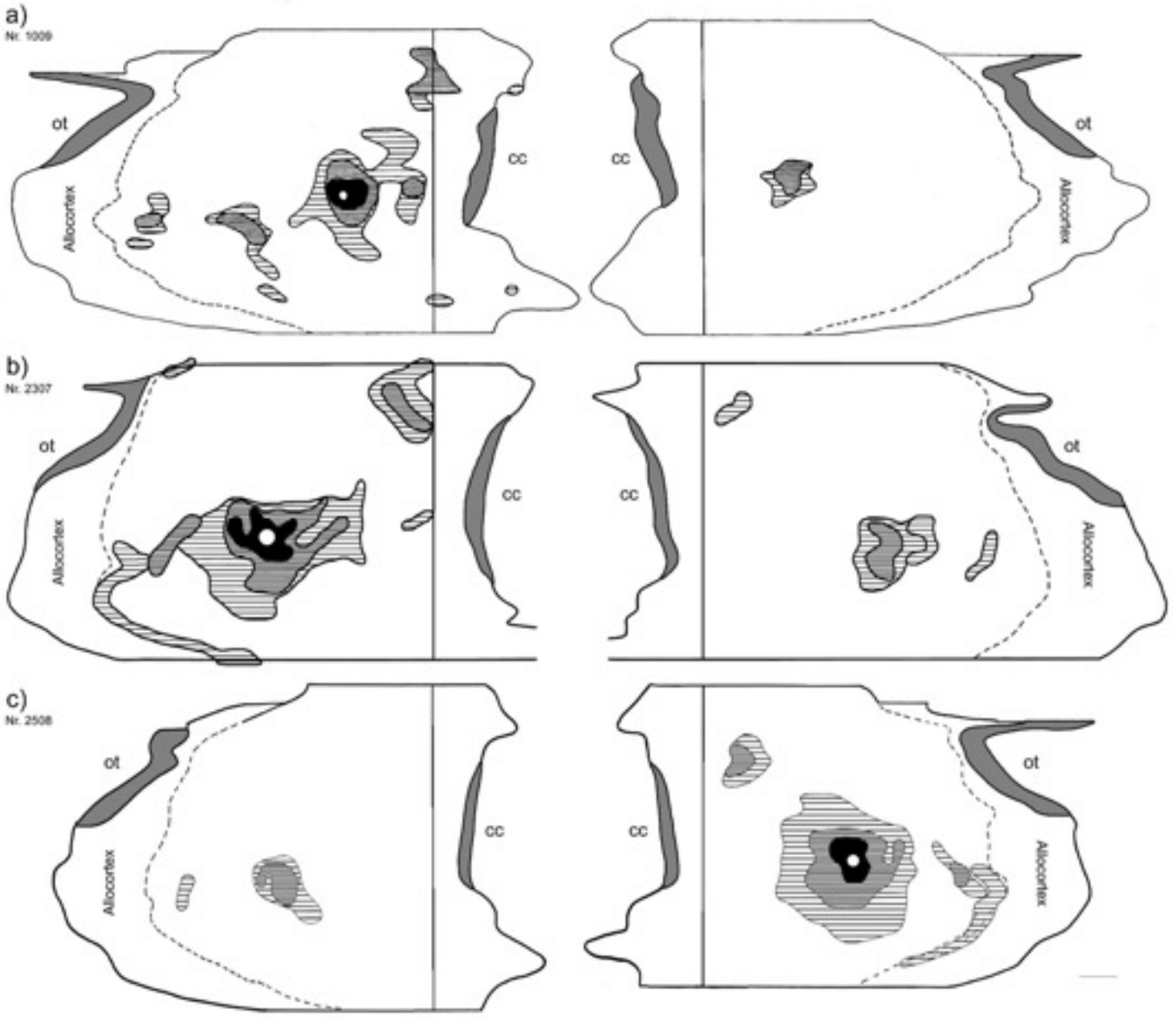

From Schüz et al., 2005

Mouse

The neurons under ≈0.1 mm^2 reach	**≈15 mm^2**
Total neocortex	**71 mm^2**
% of neocortical surface area	**20 %**

From Schüz et al., 2005

	Mouse	Monkey
The neurons under ≈0.1 mm^2 reach	**≈15 mm^2**	**≈120 - 240 mm^2**
Total neocortex	**71 mm^2**	**6400 mm^2** (Filimonov)
% of neocortical surface area	**20 %**	**2 – 4 %**

From Schüz et al., 2005

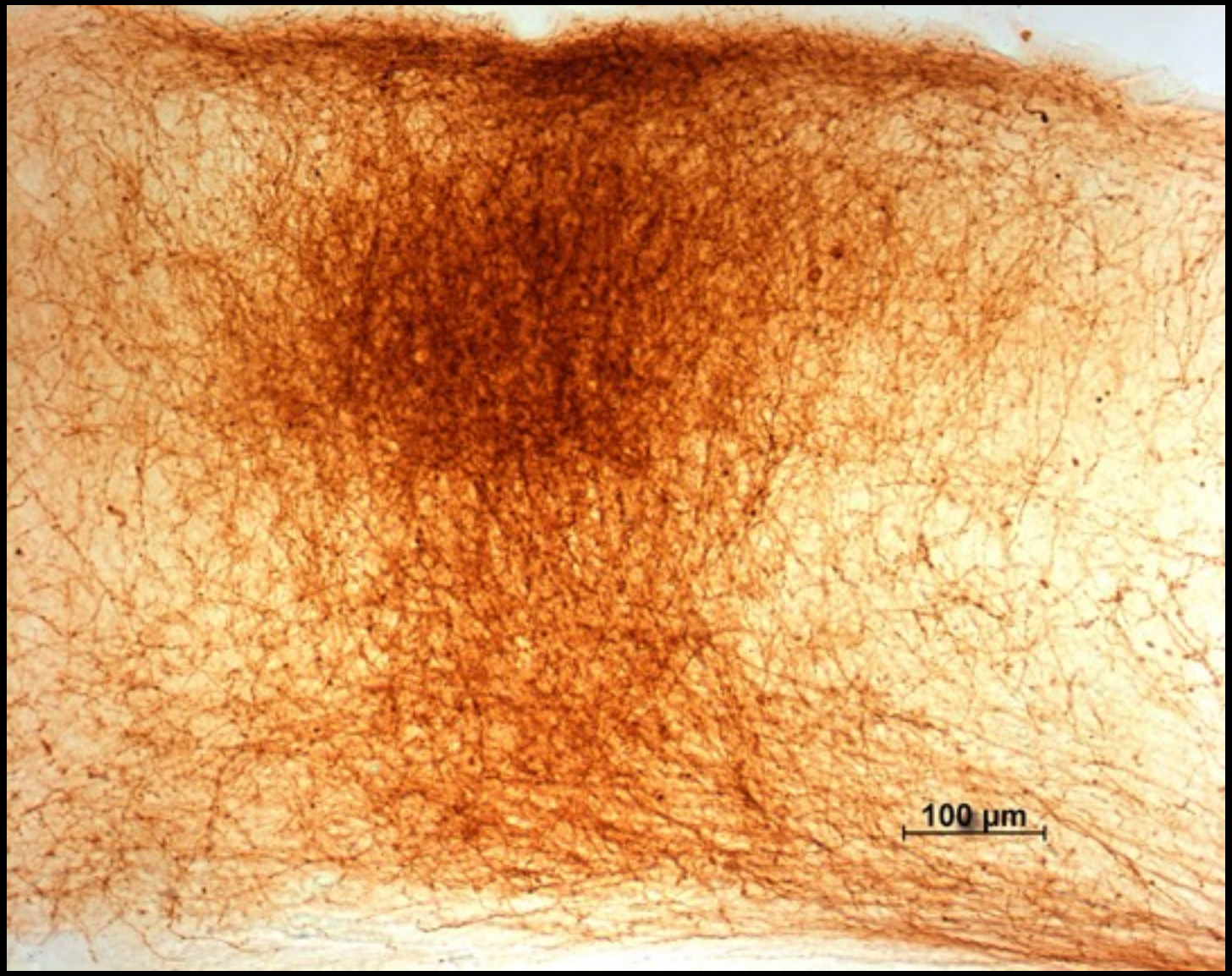
100 µm

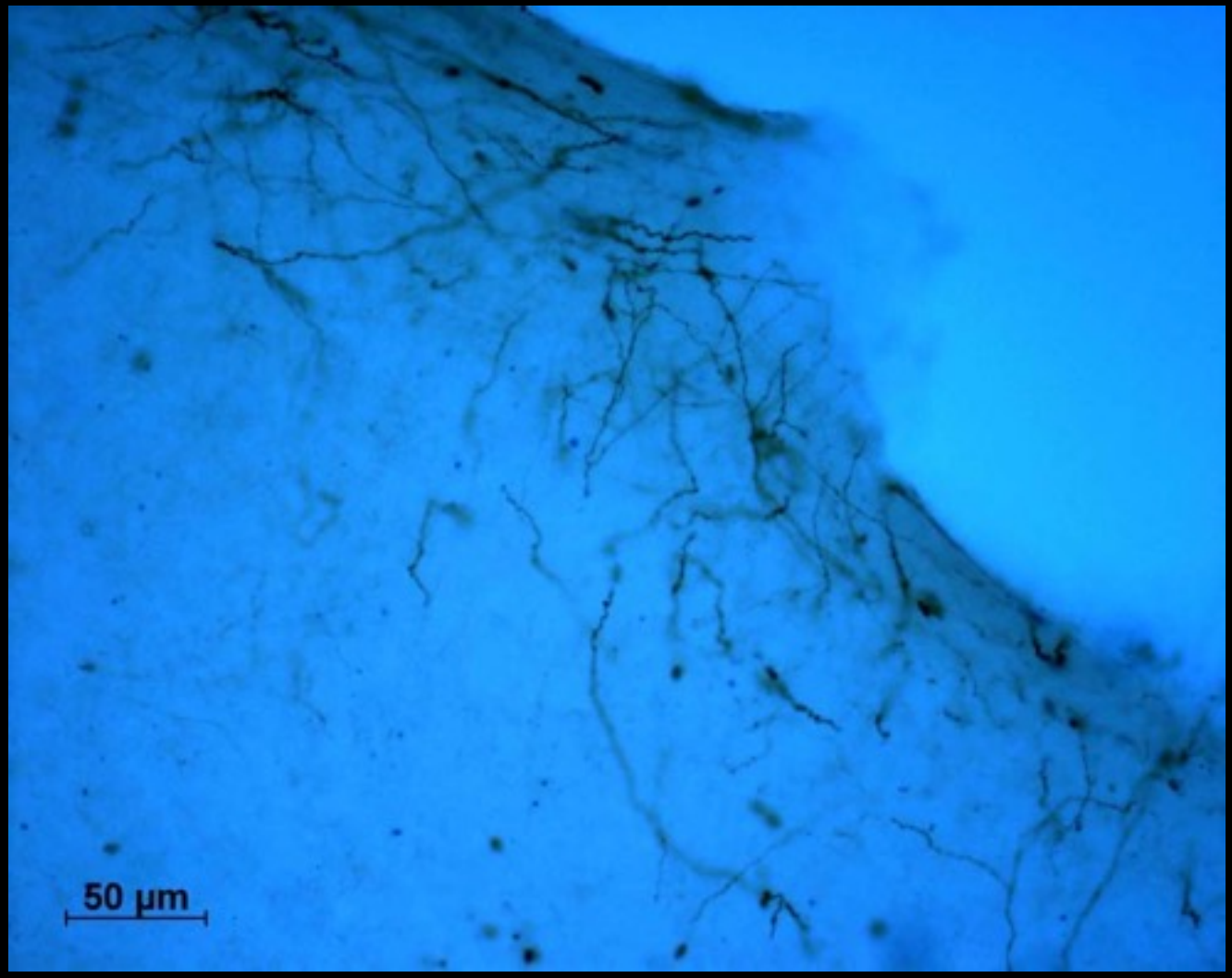
50 µm

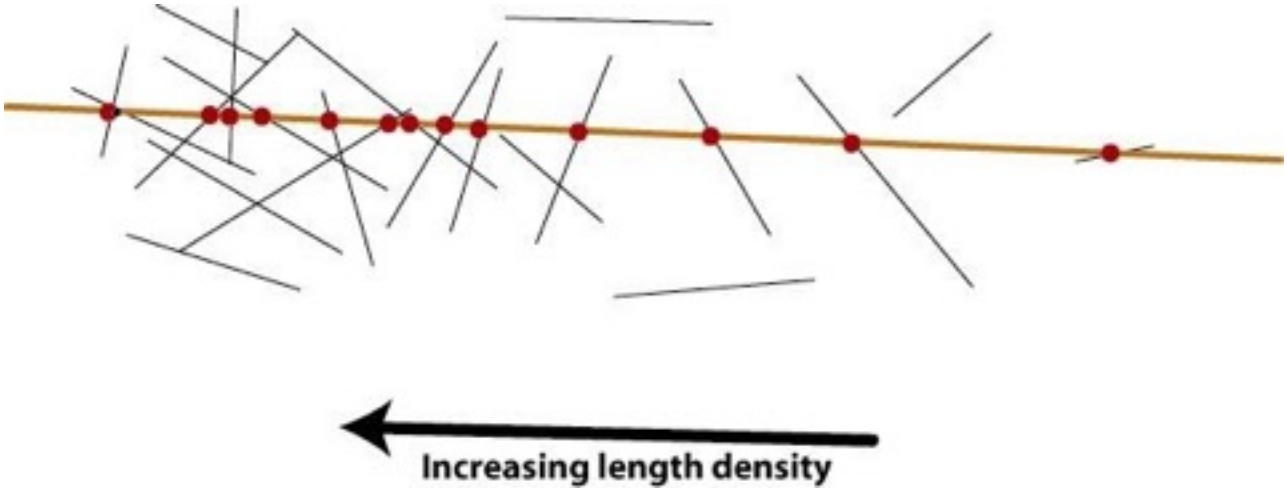

From Denis Chaimow

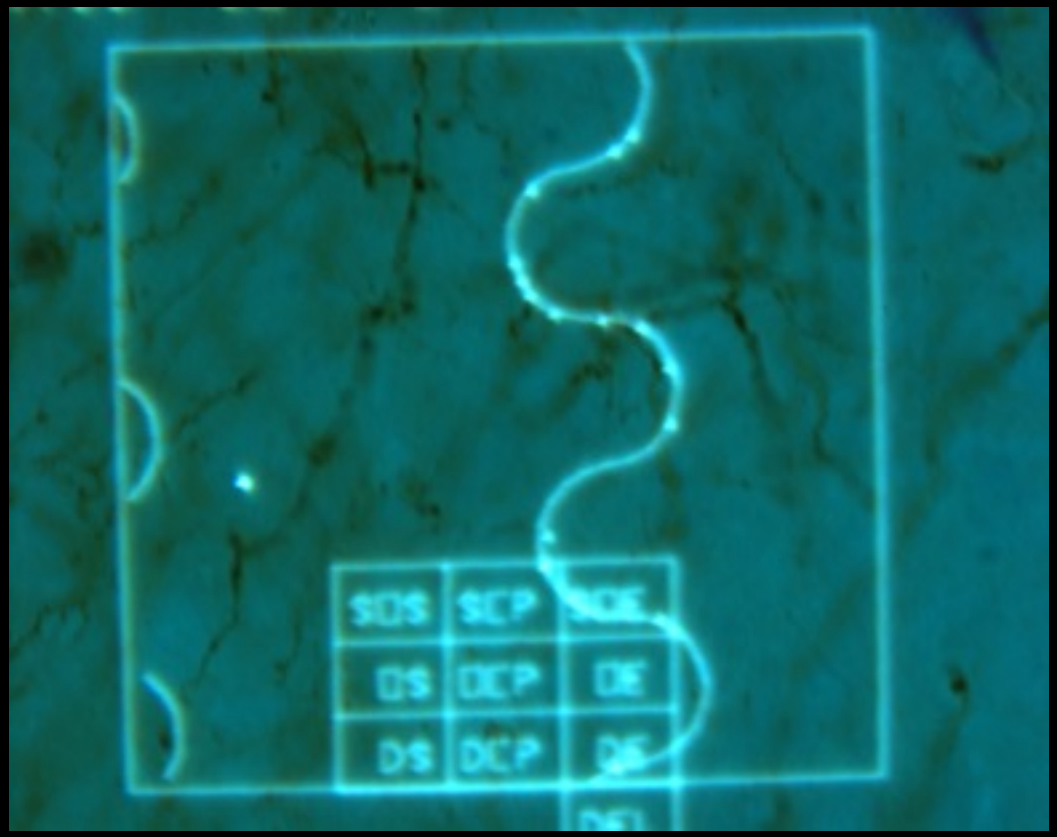

From Denis Chaimow

Fibre length per area

$$L_A = \frac{p}{2} \cdot \frac{N}{l_{testline}}$$

(Buffon, 1777; Smith and Guttmann, 1953)

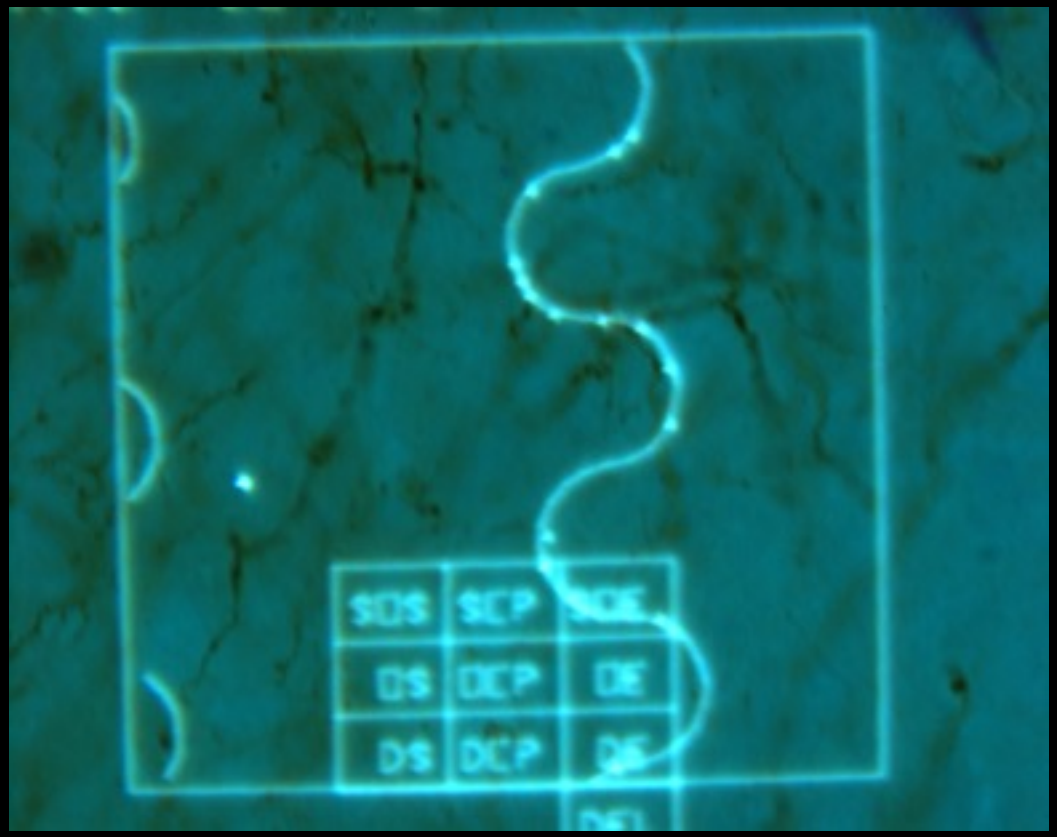

From Denis Chaimow

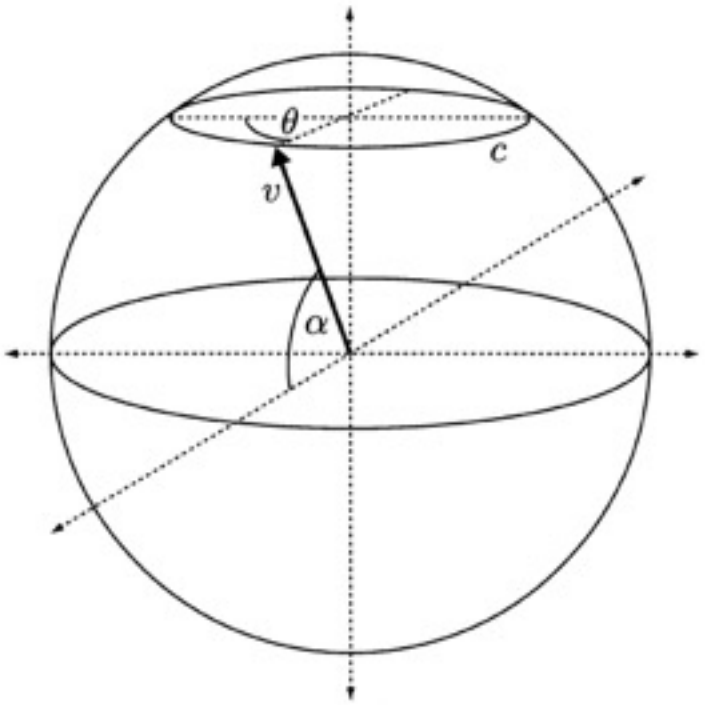

Figure 9. A 3-dimensional orientation can be represented by a vector *v* on a sphere that is parametrized by an angle of elevation α and an azimuthal angle θ. For a uniform distribution of 3-dimensional orientations, the probability density for finding a vector *v* is equal at any place on the sphere. Given a specific elevation α, *v* is constrained to lie on the circle *c*, which is the horizontal section of the sphere at the elevation α. The probability density for any vector to lie on that circle is proportional to its circumference, which is proportional to cos α. Therefore the probability density of finding a vector *v* with an elevation α in a uniform distribution of orientations is proportional to cos α.

$$\left\langle \frac{l_{2D}}{l_{3D}} \right\rangle = \int_0^{\frac{\pi}{2}} \cos(\alpha) P(\alpha) d\alpha = \int_0^{\frac{\pi}{2}} \cos^2(\alpha) d\alpha$$

$$= \frac{\pi}{4}$$

N = number of intersections
l = length of test line

$$L_A = \frac{\pi}{2} \times \frac{N}{l_{testline}}$$

d = diameter of section (50 mm)

$$L_V = \frac{L_A}{d} \times \left\langle \frac{l_{2D}}{l_{3D}} \right\rangle^{-1} = \frac{1}{d} \times \frac{\pi}{2} \times \frac{N}{l_{testline}} \times \frac{4}{\pi}$$

$$= \frac{2N}{l \times 50 \mu m}$$

From: Denis Chaimow

Low density: 3 m/mm^3

High density: 25 m/mm^3

Low density: 3 m/mm^3

High density: 25 m/mm^3

Total density of axons in the neuropil:

4 km/mm^3

25 m/mm^3 are 0.6 % of 4 km

Fibre density in the local (=black) field

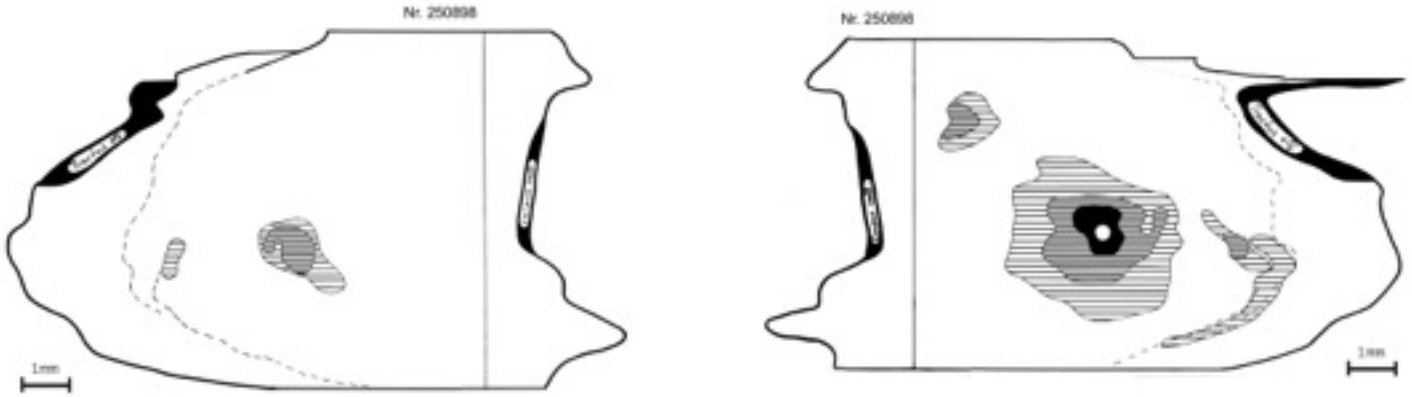

Procedure:

1) Estimating the total length of stained fibres
   (assuming 35 mm of axon per neuron)
2) Estimating the fibre length in the hatched regions
3) Subtracting (2) from (1)

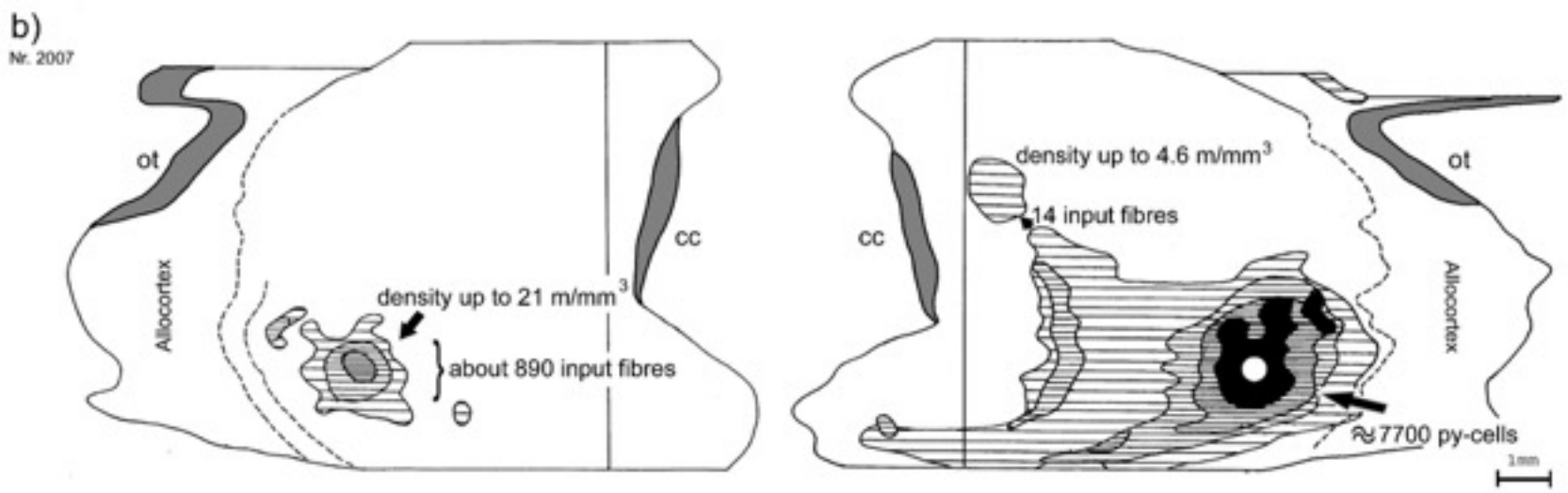

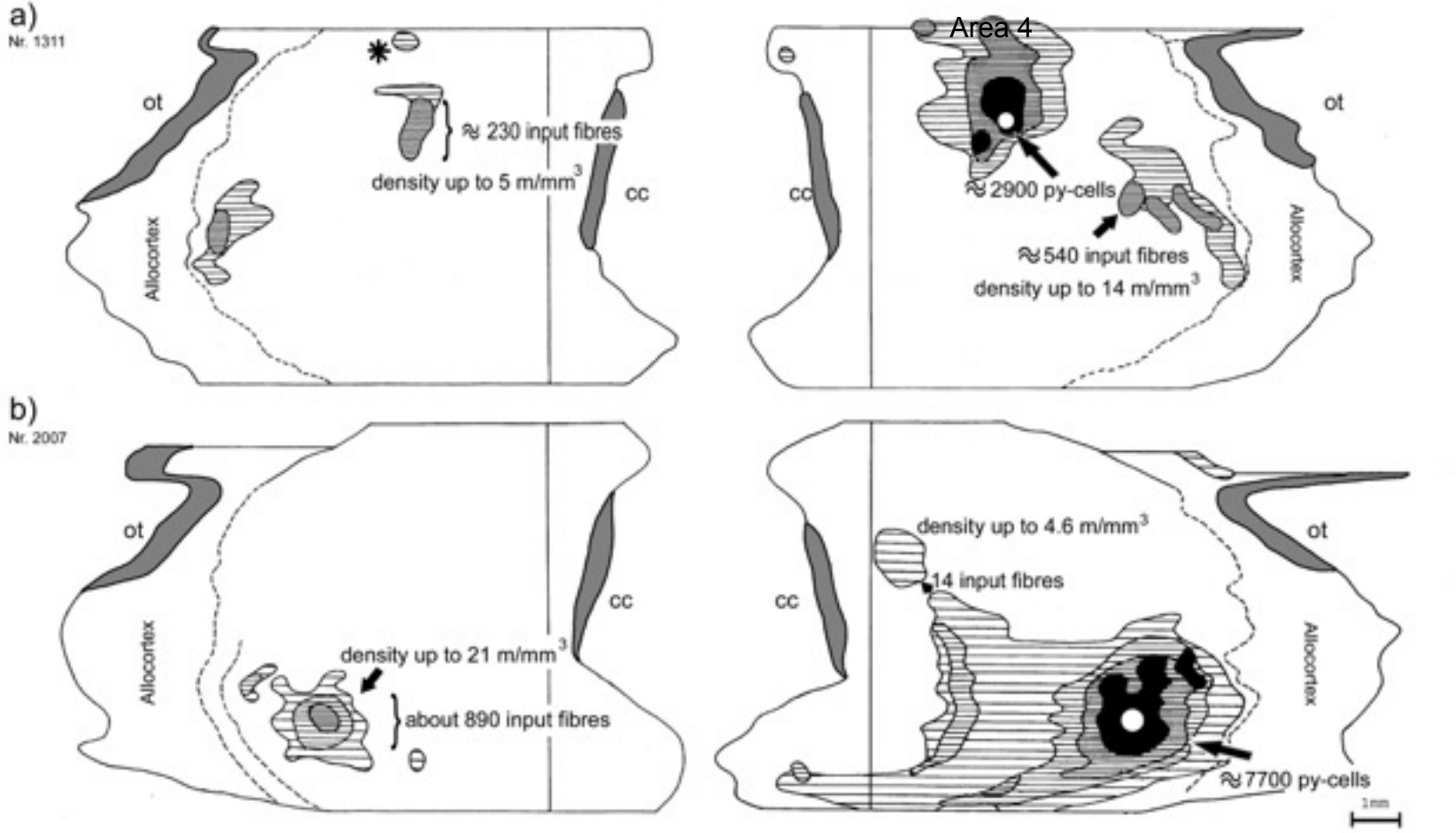
a)
Nr. 1311
ot
≈ 230 input fibres
density up to 5 m/mm3
cc
Allocortex
Area 4
ot
cc
≈ 2900 py-cells
≈ 540 input fibres
density up to 14 m/mm3
Allocortex
b)
Nr. 2007
ot
cc
Allocortex
density up to 21 m/mm3
about 890 input fibres
density up to 4.6 m/mm3
14 input fibres
ot
cc
Allocortex
≈ 7700 py-cells
1 mm

Area 41

Density in the vicinity of the injection site:

38 - 141 m/mm^3 (1 - 3.5% of 4 km)

Connectivity in the horizontal plain

Measurements	deduced numbers	Conclusions
mouse		
0.07 mm^2 project onto about 12 mm^2	(factor of > 100)	great spatial divergence
density of distant proj. 3 – 25 m/mm^3	< 1% of 4 km/mm^3	projections very weak
		great spatial convergence
Density locally 38-141 m/mm^3	a few percent of 4 km/mm^3	great mixing of inputs at any given place
2/3 of the terminal field Within a few mm of the injection site		short-range input dominating
		most projections within an area and betw. neighbouring areas

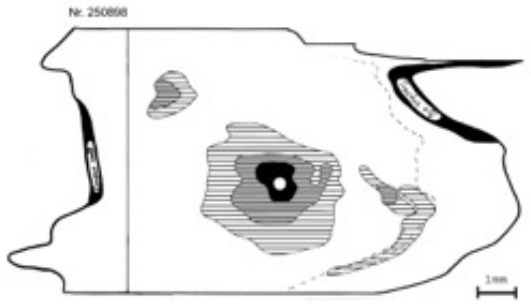

Main conclusions on horizontal connectivity:

1) Great spatial divergence of projections (> x 100 in mouse)

2) A high degree of convergence at any place

3) The largest part of the terminal field (~ 2/3) connects neurons within the same area and in neighbouring areas

Patchy connections in large brains

Together with Nicole Voges, Ad Aertsen, Stefan Rotter

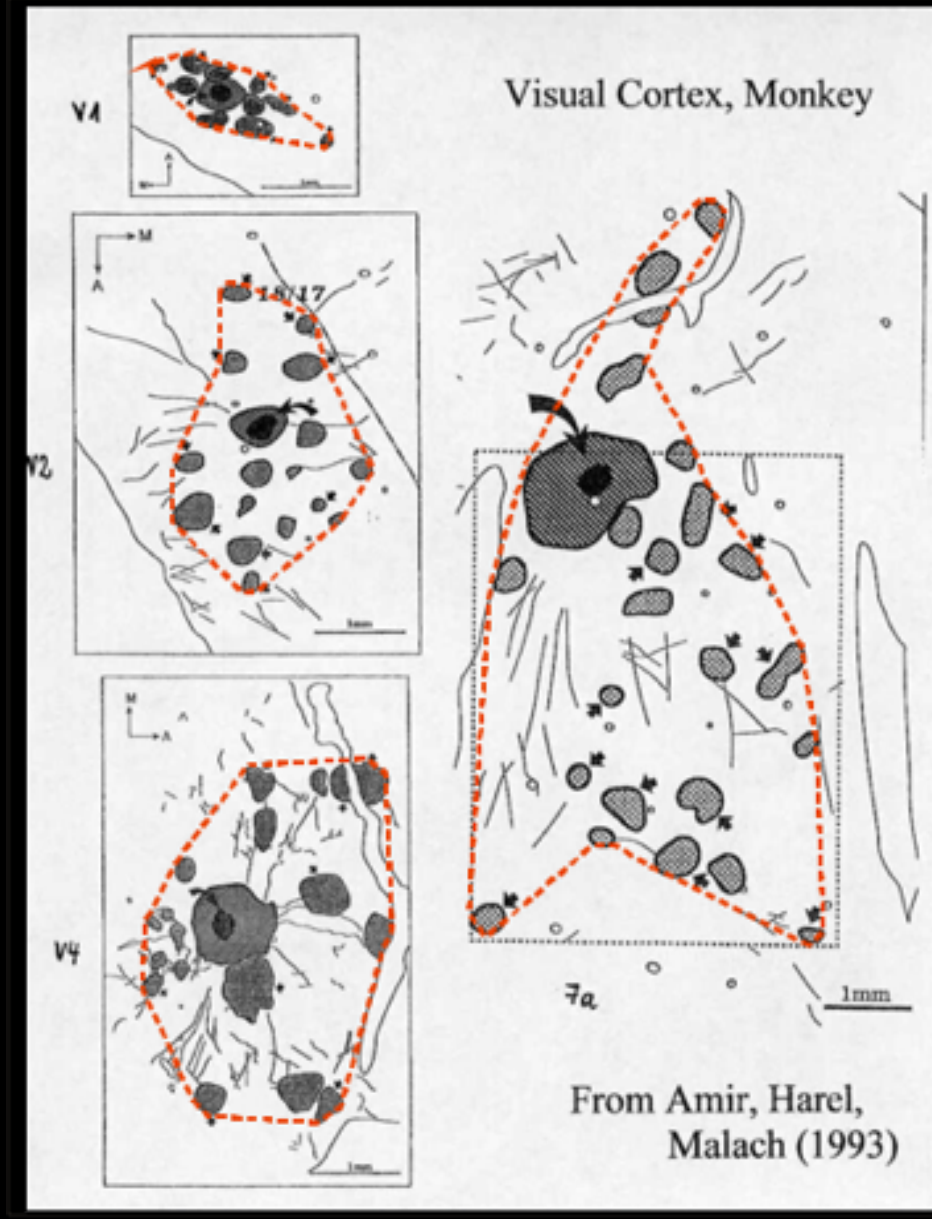
Visual Cortex, Monkey
V1
V2
V4
7a
1mm
From Amir, Harel,
Malach (1993)

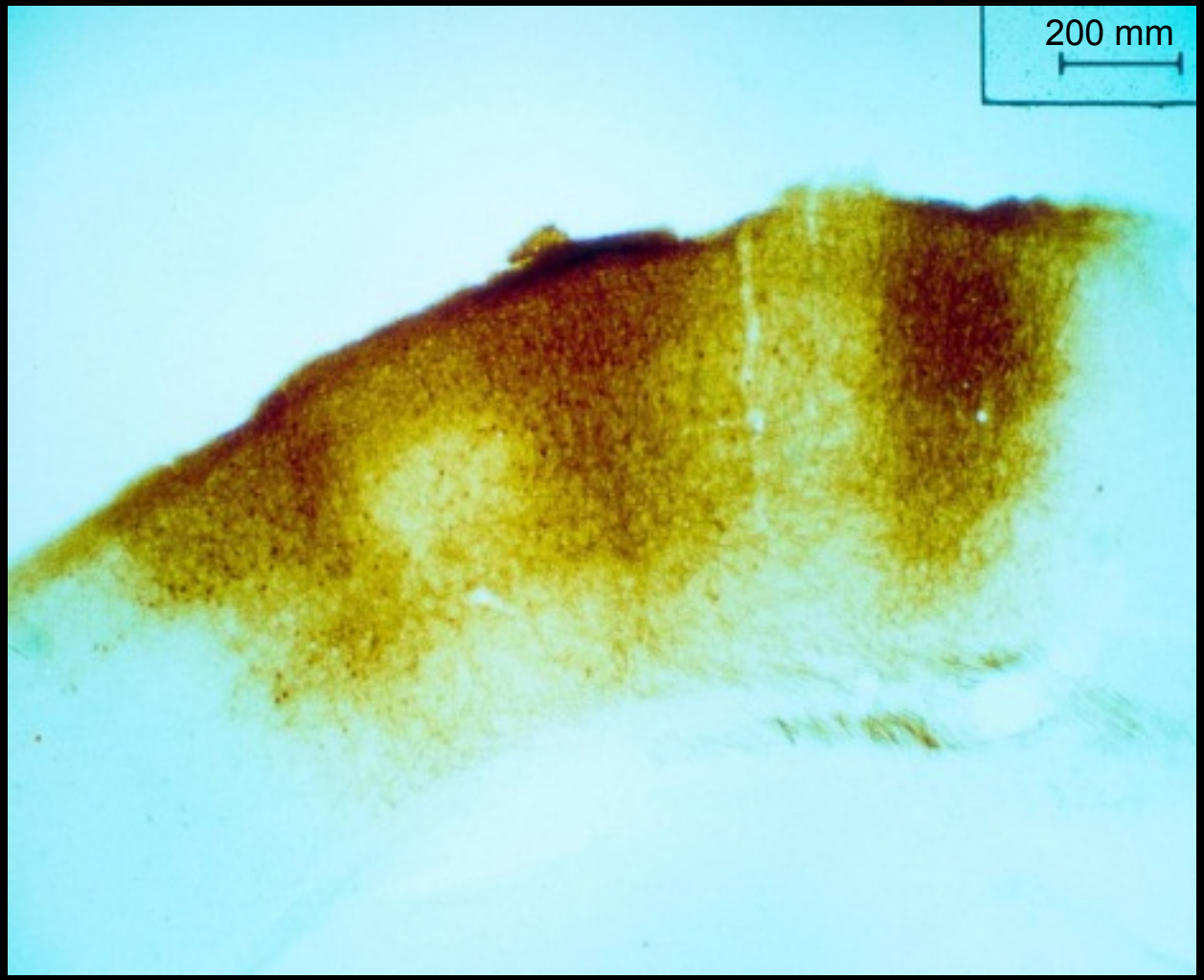
200 mm

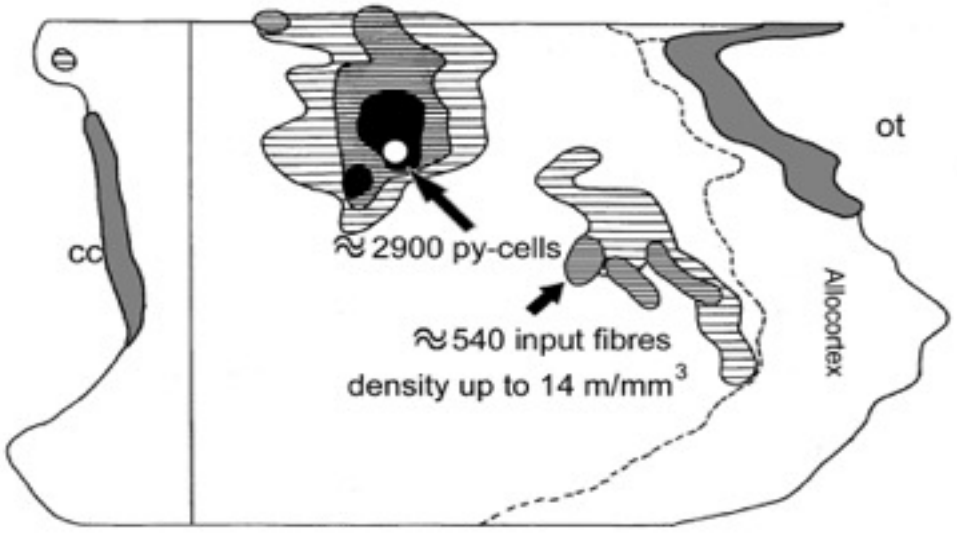
cc
≈2900 py-cells
≈540 input fibres
density up to 14 m/mm3
ot
Allocortex
1 mm

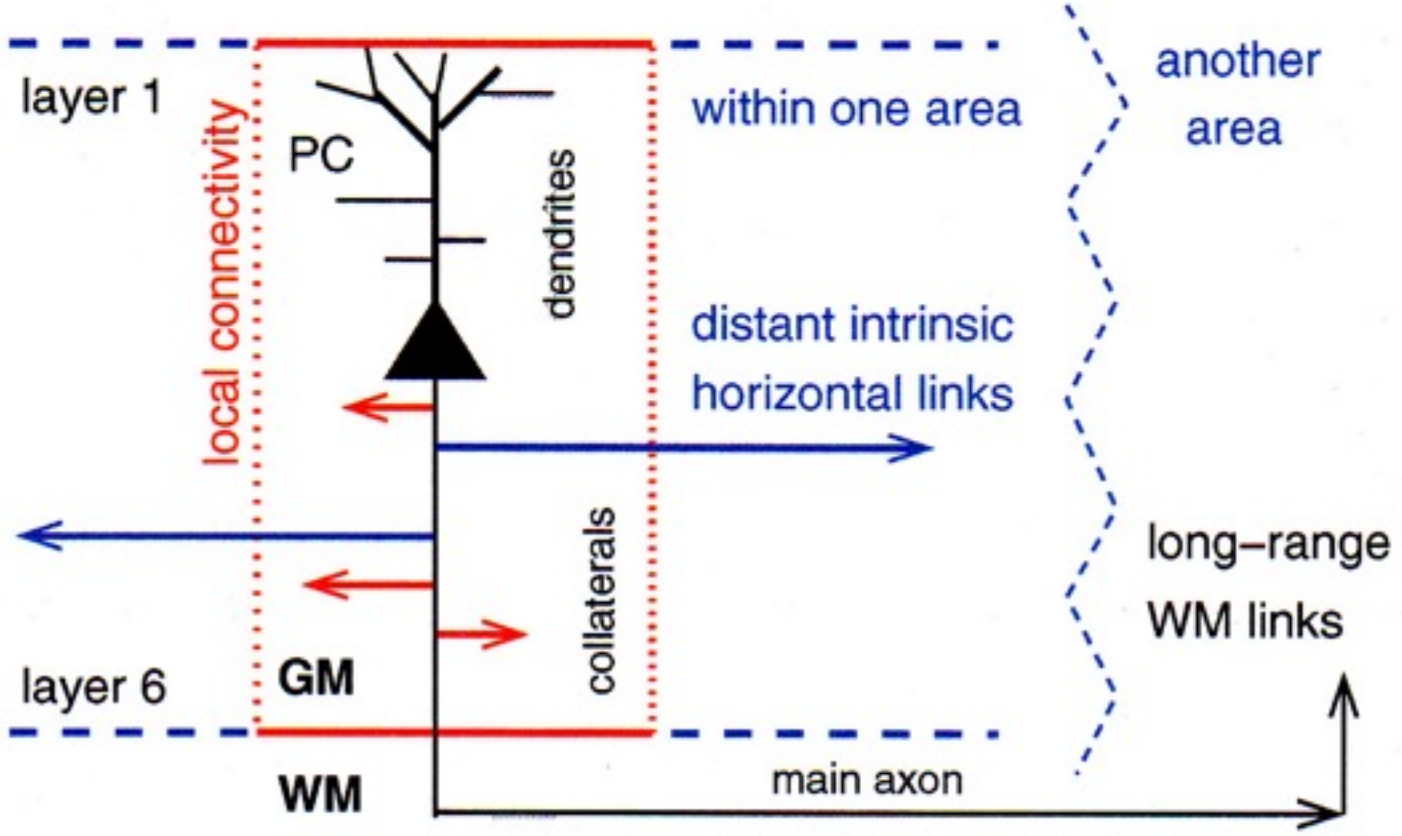

From: Voges, Schüz, Aertsen, Rotter; Progress in Neurobiology (2010)

What is the variability of these patches?

Is it possible to make a generalized model?

Literature	Species	cortical area	σ	N_p	$\varnothing_p$	d_p	$d_{p,max}$ (Σ)	d_{cc}
Gilbert & Wiesel (1989)	cat	V1	0.2				2 (6-8)	
Buzas et al. (2006)	cat	vis.	0.15		0.25	1.2, 2.1	3	
Read et al. (2001)	cat	A1 (intr.)					1.5	
Wallace et al. (1991)	cat	A1		3-8	0.8-2	0.5-6		1
Burkhalter & Bernado (1989)	human	V1, V2	0.25-1		0.3-0.5		6	0.6-1
Galuske et al. (2000)	human	22, A1 (intr.)	0.4	10-58, 30-50	0.56-0.86, 0.39-0.43		7, 5	1-1.5, 0.87-0.95
Bosking et al. (1997)	tree shrew	V1 (intr.)	0.2		0.2x 0.4	>0.5		

Table 1: List of publications on patchy projections resulting from extracellular tracer injections ('group data'), ordered according to the analyzed species and cortical areas. Listed are the injection size σ, the average number of patches per cell/axon N_p, the average patch diameter $\varnothing_p$, the average and maximum lateral distance between the cell body and the patches $d_p, d_{p,max}$, the maximum lateral axonal spread Σ, and the average distance between the patches d_{cc} (all length measurements in millimeters).

Literature	Species	cortical area	σ	N_p	$\varnothing_p$	d_p	$d_{p,max}$ (Σ)	d_{cc}
Burkhalter & Charles (1990)	rat	V1, V2	0.1-0.25		0.15-0.25		1.8	
Rumberger et al. (2001)	rat	V1, V2 (intr.)	0.3-0.6	1-3	0.37, 0.43, 0.46			0.75, 0.9
Malach et al. (1997)	owl monkey	V5 (intr.)	0.15-3.5	>29	0.3-0.5			max= 1.8
Pucak et al. (1996)	monkey	PFC	0.35	12	0.25	2.8	7.5 (9.5x5.1)	
Levitt et al. (1993)	macaque	PFC (intr.)	0.2-0.4		0.27		7-8	0.5-0.6
Lund et al. (1993)	macaque	PFC (intr.)	0.2-1.5		0.27		(9.4x3)	0.54
"	"	V1,2,4 (intr.)	0.2-1.5		0.23, 0.34, 0.35		4-6	0.43, 0.64, 0.68
"	"	SI, 4 (intr.)	0.2-1.5		0.4, 0.48		(7x6, 4.7x5.2)	0.73, 0.54
Amir et al. (1993)	macaque	V1,2, V4,7a (intr.)	0.13-0.9	5-11, 15-33	0.23-0.31	0.65-2.21	2.14-8.98	0.61-1.56

Table 2: List of publications on patchy projections resulting from extracellular injections, continuation of Table 1.

Literature	Species	cortical area	σ	N_p	$\varnothing_p$	d_p	$d_{p,max}$ (Σ)	d_{cc}
Levitt et al. (1994)	macaque	V2 (intr.)	0.2-0.3	10-15	0.25-0.3	2	4	0.25-2.2
Rockland & Knutson (2001)	macaque	V1 (intr.)			0.1		8	
Stettler et al. (2002)	macaque	V1, V2	0.2				(7)	0.75
Tanigawa et al. (2005)	macaque	V1, TE	0.23-0.54	5-21, 9-43	0.25x0.39, 0.35x0.55	0.9-2, 2.5-7.7		0.63, 1.3

Table 3: List of publications on patchy projections resulting from extracellular injections, continuation of Tables 1 and 2.

Literature	Species	cortical area	layer	N_p	$\varnothing_p$	d_p	$d_{p,max}$ (Σ)	d_{cc}
Gilbert & Wiesel (1983)	cat	vis. (intr.)	2-6		0.2-0.3	2	4	1
Martin & Whitteridge (1984)	cat	V1 (intr.)	2-5		0.1	0.2-2.2		1
Kisvarday et al. (1986)	cat	V1 (intr.)	3		0.3-0.4	0.5-1	2	
Gabbott et al. (1987)	cat	V1	5/6	3		1.1-2.6		
Binzegger et al. (2007)	cat	V1	2-6	0-5	0.35-0.6	0.1-1.5	0.21	
Ghosh et al. (1988)	cat	4γ (intr.)	2/3, 5	3-8			1.5	
Ojima et al. (1991)	cat	A1 (intr.)	2/3	2-4		0.5-2.5		
Ojima et al. (1992)	cat	A1	5/6			0.5-4.5		
McGuire et al. (1991)	macaque	V1 (intr.)	3	4			2	0.4
Lohmann & Rörig (1994)	rat	V2 (intr.)	2/3		0.18		1.2	0.2

Table 4: List of publications on 2D or 3D reconstructions of single patchy PC projections, ordered according to the species and the cortical area they refer to. Listed are the layers, the average number of patches per cell/axon N_p, the average patch diameter $\varnothing_p$, the average and maximum lateral distance between the cell body and the patches $d_p, d_{p,max}$, the maximum lateral axonal spread Σ, and the average distance between the patches d_{cc}. All measurements are given in millimeters. Part one: intracellular injections.

Literature	Species	cortical area	layer	N_p	$\varnothing_p$	d_p	$d_{p,max}$ (Σ)	d_{cc}
DeFelipe et al. (1986)	macaque	SI, motor cortex	WM	1-5			6	
Rockland & Virga (1989)	macaque	V2 to V1		1-3	0.3-0.5	0.6-4.3		0.36-0.65
Rockland & Virga (1990)	macaque	V1 to V2		1-3	0.2-0.35			0.2-0.5
Rockland (1995)	macaque	V2 to V5		1-3	0.2-0.4			0.2-0.6
Tyler et al. (1998)	macaque, marsupial	V1 (intr.)	2/3		0.32, 0.23			0.55, 0.4
Kisvarday & Eysel (1992)	cat	V1 (intr.)	3	4-8	0.4	0.5-2.8	2.8 (4.9)	1.1
Clarke et al. (1993)	cat	A1					2-7	
Wallace et al. (1991)	ferret	A1	2/3	6	0.3-0.8	1-4		

Table 5: List of publications on 2D or 3D reconstructions of single patchy PC projections, continuation of Table 4. Part two: extracellular injections with single axon reconstructions.

Results for single neurons (i.e. from intracellular injections):

	Average (Max)
-Number of patches	1 – 5 (8)
-Radius of local spread	300 – 500 mm
-Diameter of patches	200 - 400 (800) mm
- Distance of patches to cell body	0.4 - 5 (7) mm
- shared patches of closely located neurons	2 - 5

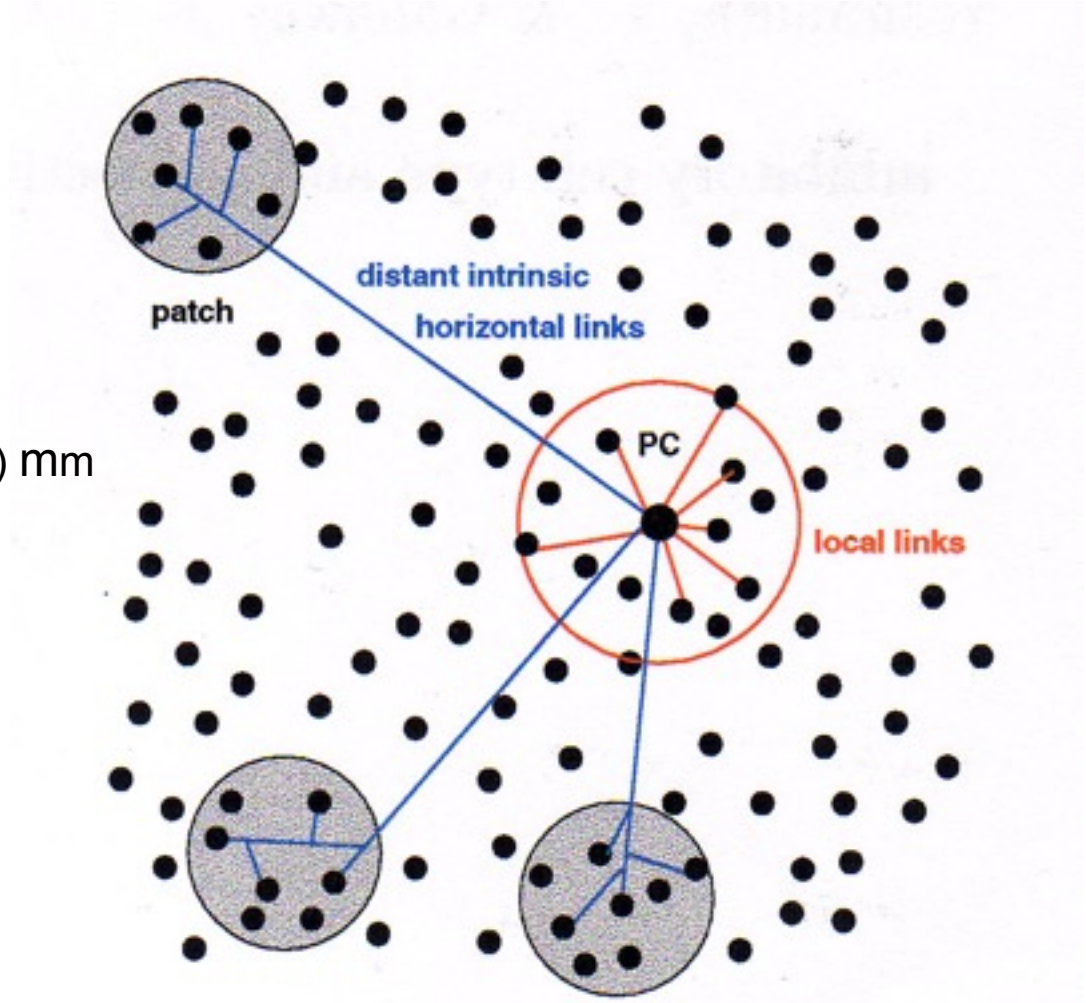

Results from extracellular injections:

Number of patches: usually 10 – 20 (total range: 1 – 58) depends on injection size and brain size, somewhat on areal hierarchy

Size of patches: comparable to those of single neurons

Distance of patches to cell body and between each other: similar as in single neurons, depending strongly on cortical hierarchy

Numbers for a model

Extracellular injections (groups of neurons):
in large brains usually 10 – 20 patches (total range: 1 – 58)
nr. depends mainly on brain size and injection size, somewhat on area

Intracellular injections	**our model**	average in diff. species/area	max	comments
single neurons:				
- Number of patches	**3**	1 - 5	8	
- Radius of local links	**0.5**	0.3 - 0.5 mm	0.5	
- Radius of patches	**0.25**	0.1- 0.2	0.4	**rather stable**
- Distance of patches to cell body	**0.75-3.75**	0.4 - 5	7	**dep. on brain size and area**
- shared patches of closely located neurons	**3 out of 6**	10 neurons shared 2 - 5 of their patches		

Result:

It is possible to make a generalized model,

which can be easily adapted to particular areas:

The size of the patches is relatively constant

The number of patches depends mainly on
- the size of the injection
- somewhat also on hierarchical level

The spread of patches depends mainly on areal hierarchy

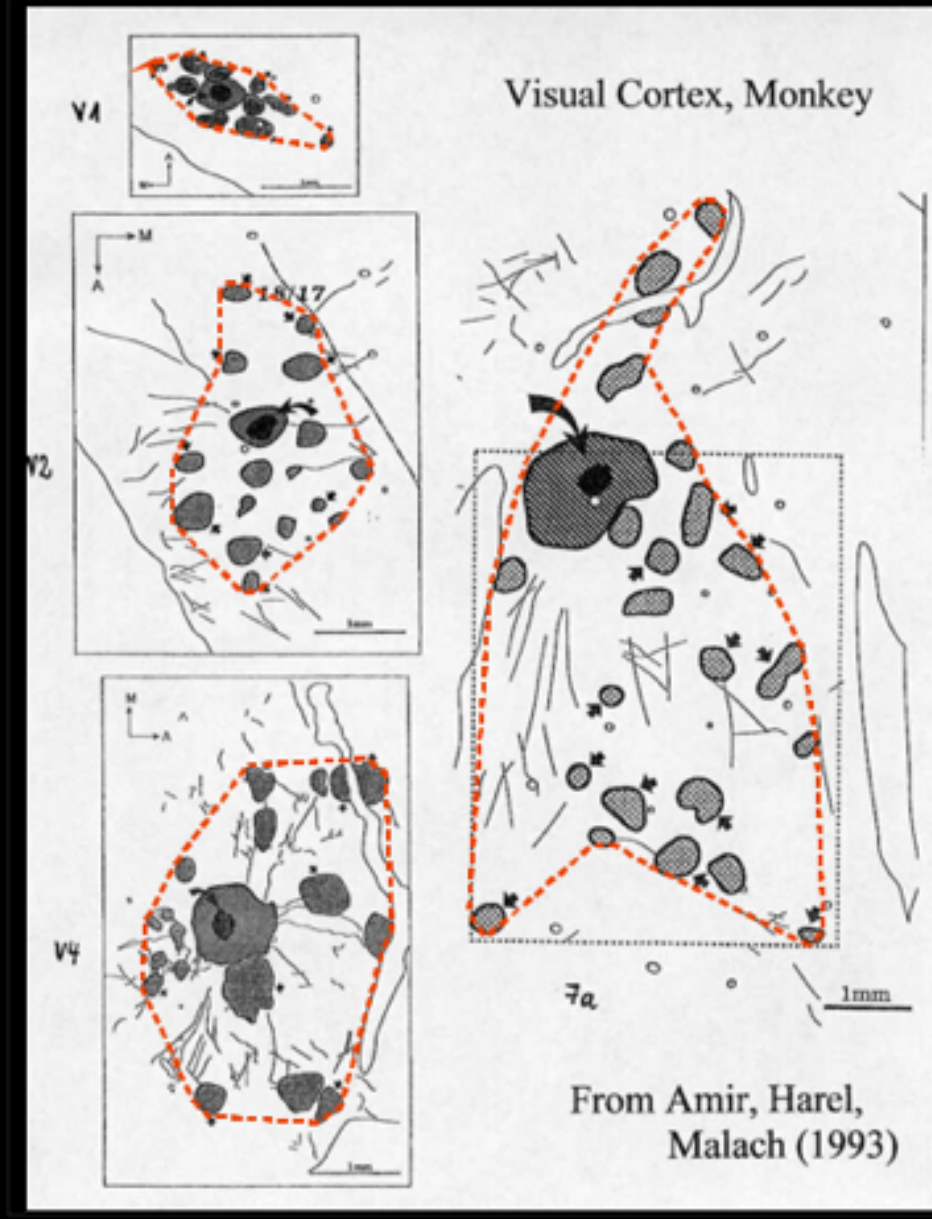
Visual Cortex, Monkey
V1
V2
V4
7a
1mm
From Amir, Harel,
Malach (1993)

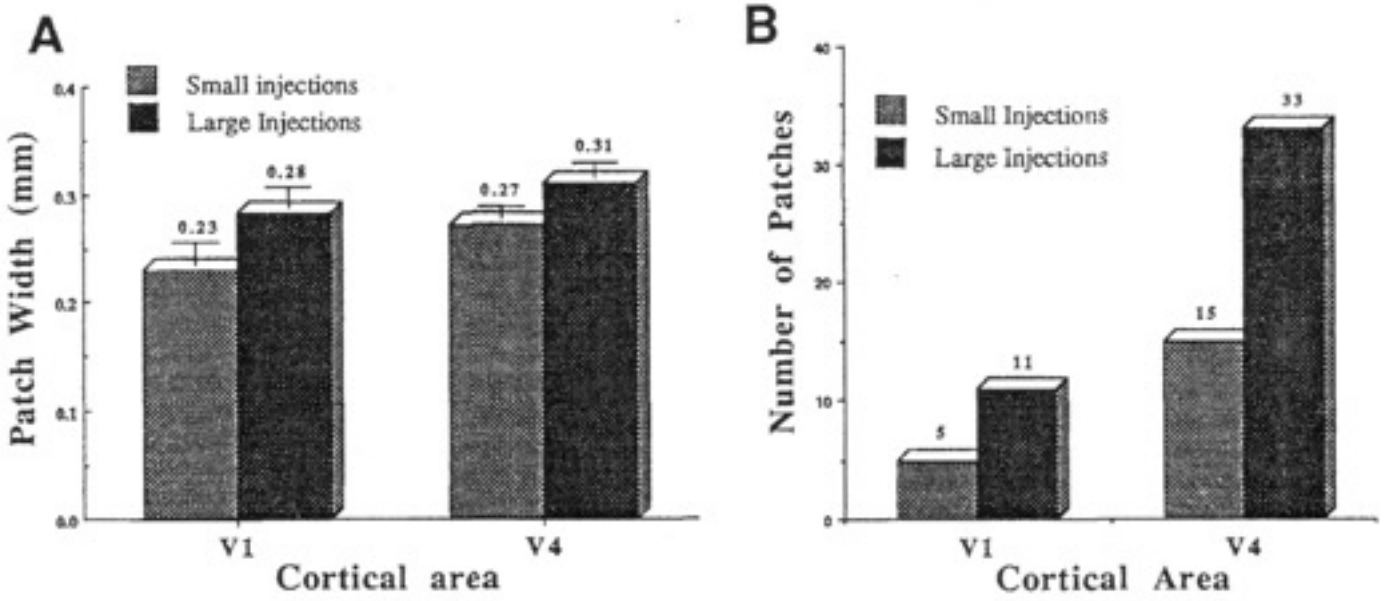

Fig. 20. Intrinsic connections produced by small vs. large biocytin injections in areas V1 and V4. **A:** Effects of enlarging the injection site on patch width. Note that patch width is barely affected by the increased injection site both in area V1 (left bars) and V4 (right bars). **B:** Effects on number of patches. Here increasing the size of injections had a marked affect. Patch number both in areas V1 and V4 more than doubled due to the increased in size of injection sites.

Amir et al (1993)

Role of patches?

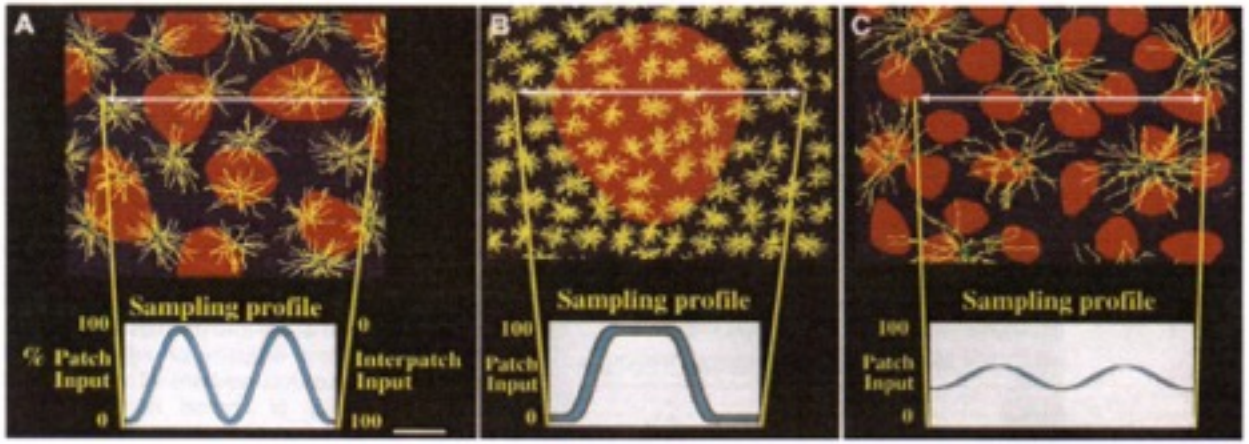

Fig. 2. *Dendritic sampling from axonal patches: macaque area V1.* **(A)** *A scheme depicting how dendritic arbors of upper-layer pyramidal neurons sample from incoming inputs clustered into patches (red). Only a few representative neurons are shown (yellow), whereas in the real tissue the area is densely packed with pyramidal neurons having highly overlapping dendritic fields. The neurons and patches were generated from examples revealed by anterograde and retrograde transport of biocytin in area V1 of the macaque monkey. Note the similarity in size of the dendritic spread of individual neurons and the width of axonal patches. In this case, only a few neurons at the center of a patch or interpatch will receive 'pure' inputs while all the others will sample different mixes of patch–interpatch inputs. Below is the population sampling profile which shows the mix of patch–interpatch inputs to each neuron along the white line. The x-axis corresponds to position along the white line, while the y-axis shows the ratio of patch–interpatch inputs. Note that the population sampling profile oscillates smoothly between pure interpatch inputs and pure patch inputs, thus generating maximum neuronal diversity. Scale bar, 100 μm.* **(B)** *Dendritic sampling from oversized axonal patches. A depiction of a hypothetical case in which the size of the axonal patches greatly exceeds the spread of dendritic arbors. Note that, in this case, most dendritic arbors will be confined either to the patch or to the interpatch compartments. Only a small fraction of the neuronal population will integrate information from both compartments. The graph below shows the population sampling profile for this case. Note that, unlike the case shown in (A), here the peaks of the population sampling profile are flattened leading to redundant sampling by neighboring neurons.* **(C)** *Dendritic sampling from undersized axonal patches. Depiction of a hypothetical case in which the size of dendritic spread greatly exceeds the width of axonal patches. Note that in this case all neurons receive mixed patch–interpatch inputs so that the range of possible mix ratios is reduced. This is reflected in the shallow population sampling profile.*

R. Malach (1994) TINS 17 (3)

Max Planck Institute for Biological Cybernetics in Tübingen. *Foto: Friedrich Förster*